

**CFD ANALYSIS OF HEAT TRANSFER ENHANCEMENT IN A FLOW HEAT EXCHANGER USING NANOFLUIDS (MWCNT/H<sub>2</sub>O, AL<sub>2</sub>O<sub>3</sub>/H<sub>2</sub>O)****Mr. Samir Govindrao Potdar <sup>a</sup>, Dr. Jai Bahadur Balwanshi <sup>b</sup>**<sup>a</sup> PhD Research Scholar, Dr. A. P. J. Abdul Kalam University, Indore – 452010<sup>b</sup> Professor, Dr. A. P. J. Abdul Kalam University, Indore – 452010**ABSTRACT**

*Motivation research for the modelling for Heat Transfer Enhancement using NanoFluids for Cooling of Electronic Components can be approached from a variety of perspectives, such as the increasing demand for high-performance electronic devices, the limitations of conventional cooling techniques, and the potential benefits of using nanofluids for cooling. Developing more efficient and effective cooling methods that can keep electronic components cold is the overall goal of the study on modeling heat transfer improvement utilizing nanofluids for cooling of electronic components up with the rising demand for high-performance electronic devices. By investigating the potential cooling benefits of nanofluids, this study may aid in the creation of more sophisticated cooling systems that can improve the performance and dependability of electronic devices. This study covers the CFD analysis. Two different types of nanoparticles for water with 0.7% concentration of Al<sub>2</sub>O<sub>3</sub> (alumina) nanoparticles and Multi-Walled Carbon Nanotubes (MWCNT) exhibited lower temperature ranges compared to pure water under similar operating conditions. Al<sub>2</sub>O<sub>3</sub> and It has been employed MWCNT with various nanoparticle sizes between 10nm and 20nm. Water has also been used for cooling purposes with volume fractions of 1%, 3%, 5%, and 7% of the various kinds of nanofluids. The analysis considered various operating conditions, including different tube diameters and discharge rates, to examine the impact on heat dissipation and temperature distribution. Contour plots of static temperature at the outlet were generated to visualize the thermal behavior within the system. The results showed that for water as the base fluid, the temperature distribution at the outlet varied with different tube diameters and discharge rates. Increasing the discharge rate generally led to a decrease in temperature, indicating improved heat dissipation capabilities. Furthermore, the inclusion of nanoparticles in water demonstrated enhanced heat transfer performance. These findings suggest that nanofluids have the potential to improve cooling efficiency and reduce the temperature of electronic components. The CFD analysis provided valuable insights into the thermal behavior of the cooling system using different fluids and operating conditions. The temperature contours offered a clear visualization of the temperature distribution within the system, allowing for the identification of regions with higher and lower temperatures. This information is crucial for assessing the effectiveness of the cooling system and evaluating the thermal performance of different fluids for electronic component cooling. Overall, the results of this study highlight the potential of nanofluids, specifically water with 0.7% concentration of nanoparticles, for heat transfer enhancement in electronic component cooling. The findings contribute to the understanding of the thermal behavior within cooling systems and provide valuable insights for the design and optimization of cooling solutions for electronic devices.*

*Keywords: CFD, Al<sub>2</sub>O<sub>3</sub>, MWCNT, Nano fluid, etc.*

**1. Introduction**

Recent years have witnessed a remarkable increase in advancement in electronic technology, leading to the miniaturization and increased power density of electronic devices. As a consequence, the demand for effective cooling techniques to dissipate heat generated by these devices has become increasingly crucial. Traditional methods of chilling, that include air or liquid conditioning, have encountered limitations in addressing the escalating thermal management challenges. To overcome these limitations, researchers have turned their attention to innovative approaches, and one such promising technique is the utilization of nanofluids for heat transfer enhancement.

Nanofluids, as the name suggests, consist of nanoparticles disseminated in conventional heat transfer fluids, such as water or oil. These nanoparticles, which typically range in size from one to one hundred nanometers, possess exceptional thermal properties that can significantly enhance heat transfer capabilities when compared to conventional fluids. By incorporating these nanoscale additives into the cooling systems of electronic components, it is possible to achieve improved thermal performance and mitigate the challenges associated with traditional cooling techniques.

Modern computers as well as electronic devices generate excessive heat, which is a significant issue. The cooling system transfers along with extracts heat from computer components. Since various A method must be in place to remove the heat produced by functioning computer components for the purpose to maintain a secure working environment. This is the function of computer radiators [1] and utilizing appropriate refrigerant fluids. The system's cooling performance will have a significant impact on the enhancement of computer components. Multiple CPUs may be cooled at once using fluid heat sinks. They concurrently cool the CPU, GPU, and processor supply circuits in addition to the main processor. In search of an efficient and integral chiller to protect their computer's internal components, many users have adopted it. Fluid heat absorbers can theoretically chill the processor to the temperature of the cooling fluid. As a result of their modest operational flow rates, these heat sinks produce commotion while operating. Furthermore, the system's noise production is kept to a minimum while employing the fan with the radiator (of the heat sink). [2].

A basic fluid is combined with nanometer-sized particles to create a nanofluid. By spreading created nanoparticles in the beginning fluid, you may increase the working fluid's thermal conductivity. The use of nanofluids rather than conventional fluids in a range of systems has been shown to improve thermal performance in several earlier investigations. Nanofluids, which include nanoparticles in liquids that are generally smaller than 100 nm in size, have become a contender for heat transfer system design. Over the last ten years, several experimental and computational research have investigated how nanofluids might improve heat transmission. [3]. Rafati et al., [2] At various Reynolds numbers, the effects of alumina nanofluid on heat transfer efficiency in central processing unit (CPU) cooling were investigated. Korpyś et al., [4] Both mathematically and experimentally, the effects of employing To evaluate a commercial heat sink for cooling PC CPUs, water and CuO nanofluids were used. Jeng et al., [5] Examine the impact of replacing distilled water in a hybrid cooling system for electronic processors with Al<sub>2</sub>O<sub>3</sub>/water nanofluid on heat dissipation performance, increased water pump power consumption, and lowered radiator surface temperature. Selvakumar et al., [6] Convective performance in an electronic heat sink was increased by 29.63% by using a 0.2% volume fraction of CuO/water nanofluid. Garg et al., [7] Researchers looked at the impact of energy dispersal on the viscosity of aqueous nanofluids containing multi-walled carbon nanotubes. It was investigated how energy dispersion affected viscosity, thermal conductivity, and laminar convective heat transfer. According to the findings, thermal conductivity and the augmentation of heat transfer increased up to the ideal period and then decreased as ultrasonication continued. CNT nanofluids,

horizontally flowing aqueous suspensions of multi-walled carbon nanotubes, were studied for their heat transfer properties by Ding et al., [8] The observed increase in convective heat transfer is contingent on flow parameters and CNT concentration. Prior research on Al<sub>2</sub>O<sub>3</sub> nanofluid, and CNT CPU cooling in particular, has been limited. To comprehend how CNT nanofluids behave during thermal transfer, more research is required. Carbon nanotube (CNT) and alumina nanofluids are proposed as new working fluids for CPU radiators in the current study. The following are the most essential aspects of the investigation: To demonstrate its superiority, the thermal performance of CNT nanofluid is compared to that of alumina nanofluid. The enhancement of nanofluid heat transfer is calculated for both carbon nanotubes and alumina. CNT nanofluids enhanced heat transmission by 13% compared to alumina nanofluids' 6% improvement. The highest CPU temperature is recorded for a variety of parameter types. CPU maximal temperature was reduced by approximately 22% with CNT and 20% with Alumina nanofluid. Harmand et al., [9] Combining a 3D thermal model with a transient model, we investigated the thermal cooling of a planar heat conduit employed to cool a number of electronic components. Li and Chiang [10] It has been investigated how a shield affects the thermal and hydraulic properties of plate-fin vapor chamber heat sinks with cross-flow cooling. Attia and El-Assal [11] The impact of working fluid surfactant on the thermal performance of vapor chambers with varying charge ratios was investigated. Ji et al., [12] Analyze the effect on the thermal efficiency of an expanded vapor chamber with an extended condenser section and an extended evaporator component. Tsai et al., [13] It was investigated how inclination affected the operation and temperature uniformity of vapor chambers. Chen et al., [14] studies on the vapor chamber's thermal resistance to sintered aluminum particles. Hassan and Harmand [15] We looked at the three-dimensional transient model for assessing the thermal performance of a vapor chamber. Egan et al., [16] analyzed thermal design space using finite element numerical simulations to understand thermal phenomena in embedded electronics design. The findings reveal that the two factors most strongly influencing the thermal performance of an integrated electronic device are substrate conductivity and exposed heat spreader surface area. Gauch et al., [17] studied system-level phase change modeling for thermal models using transient analysis & conventional material attributes. In a case study, three different versions of a system-level CFD model of an electronic enclosure without PCM along with PCM retrofitted were created Kitamura et al., [18] In electronic enclosures, the impact of air conditioning on natural convection heat transfer was investigated. The ramifications of casing inclination on casing temperature increase were shown using experimental and computational results. A thermal design reference that the corporation acquired explains how increasing the angle of inclination enhances the cooling effect. Nakayama et al., [19] The effects of component location on junction temperature have been quantitatively examined. They discussed experimental methods for testing the predictions as well as the CFD analytical approach for the development of the heat sink and duct. Leon et al., [20] Through the numerical analysis of three different models, it was possible to calculate the ratio among the heat evacuated and the energy used during the refrigerant's transit through the cooling fins. Consistently maximizing heat transfer flux requires the use of a split heat sink. The effect of nanofluids on desktop computers' CPU is examined in this research.

Choi [3] presented nanofluids for the first time as suspensions of nanoparticles in typical working fluids including water, ethylene glycol, and motor lubricants. The thermophysical characteristics of the working fluids are enhanced by the addition of particles having better thermal conductivity than the basic fluids. Since then, this property has attracted the attention of other researchers, who hope to harness the positive traits of this newfound class of working fluids for a variety of applications [21] [22] [23] [24].

By adding nanoparticles like carbon nanotubes and oxide as well as non-oxide particles to combustion fluids, researchers have tried to improve the thermophysical characteristics of thermal lubricants. One of the most important features of thermal lubricants is viscosity. There aren't many academic articles on this

subject, [25]. SiO<sub>2</sub> and MWCNT are being investigated in terms of their rheological properties as oil-based nanofluids. by Hemmat et al. [26]. Their results demonstrated that the nanofluid under study is a Newtonian fluid in which its dynamic viscosity increases as particle concentration increases. Asadi and Asadi [27] At different temperatures and solid concentrations, the viscosity behavior of a ZnO-MWCNT/oil hybrid nanofluid was studied. Across the investigated spectrum of shear rates, temperatures, and solid concentrations, the synthesized nanooil exhibited Newtonian behavior. In addition, they presented a novel connection for predicting the nanofluid's dynamic viscosity. In a distinct experiment, Al<sub>2</sub>O<sub>3</sub>-engine oil nanofluids were examined for their dynamic viscosity at various temperatures and solid concentrations. Hemmat et al. [28]. Their research indicates that the nanofluid produced is a Newtonian fluid with a viscosity that increases with solid concentration. The largest increase was approximately 132% greater than that of refined oil. Further investigation was conducted by Hemmat et al. [29], The viscosity of a non-Newtonian nanofluid containing TiO<sub>2</sub> particles was examined at various temperatures (from 25 to 50 degrees Celsius) and solid concentrations (0.125 to 1.5 percent). The dynamic viscosity of nanofluids can now be predicted due to the establishment of an original correlation. Additionally, they discovered that the nanofluid's viscosity responds to changes in solid concentration more rapidly. Asadi et al. [30] The viscosity of an oil-based nanofluid containing magnesium oxide particles was investigated. According to their research, nanofluid is a Newtonian fluid whose viscosity increases with solid concentration and decreases with temperature. When choosing a thermal lubricant, it is also important to consider its thermal conductivity. Despite extensive research, there is much to learn about the thermal conductivity of different nanofluids. [31], [32], [33], Oil-based nanofluids' thermal conductivity has not yet been properly researched. [34], [35]. The thermal conductivity of oil-derived nanofluids has not yet been thoroughly studied. Etefaghi et al. [36]. Across a narrow range of solid concentrations (0.1 to 0.5 wt%), the thermal conductivity of the original fluid increased during experiments content increased. At a strong concentration of 0.5% by weight, the maximum rise was about 23%. Aberoumand and Jafarimoghaddam [37] We examined the thermal behavior of Cu-engine oil nanofluid over a broad temperature range (313 K to 380 K) and a constrained range of solid concentrations (0.5% to 1%). The nanofluid's thermal conductivity reached a maximum of 31% at a solid concentration of 1% as well as a temperature of 380 K. In a particular study conducted by, Aberoumand et al. [38], The experimental investigation of the thermal conductivity of silver-particle-containing nano-oil. They discovered that as temperature and solid concentration boosted so did the nanofluid's thermal conductivity. In addition, they showed a novel correlation for predicting the thermal conductivity of nanofluids in the studied concentration and temperature ranges.

From the above literature review, it can be deduced that the research deficit in the study of nanofluid cooling for electronic components stems from a number of important areas that require further study. First, despite the fact that computational simulations have yielded promising results, there is a paucity of extensive experimental validation to confirm the accuracy and dependability of these simulations. This divide would be bridged and a more robust understanding of nanofluid cooling performance would be attained by conducting exhaustive experimental studies with diverse configurations, operating conditions, and measurement methods. The dynamic viscosity as well as thermal conductivity of an Al<sub>2</sub>O<sub>3</sub>-MWCNT nanofluid at various temperatures were examined in the current work. There have been given two novel correlations between temperature as well as solid concentration, dynamic viscosity and thermal conductivity. likewise distinct figures of merit for internal laminar & turbulent flow phases have been used to evaluate the nanofluid's ability to transport heat. Finally, it has been hypothesized how the inclusion of nanoparticles may affect the convection heat transfer coefficient and pumping power.

## 2. Methodology

The methodology for studying nanofluid cooling for electronic components typically involves a combination of experimental and computational approaches. In parallel, computational simulations are performed employing numerical techniques such as computational fluid dynamics or finite element analysis. These simulations involve developing mathematical models that describe the fluid flow and heat transfer phenomena occurring in the nanofluid cooling system. The properties of nanofluids, obtained from experimental measurements or established correlations, are incorporated into the models. By varying the input parameters, simulations are conducted to analyze the impact of factors like nanoparticle concentration, size, and fluid flow characteristics on cooling performance. Experimental data are contrasted with the computational findings to validate the accuracy and reliability of the models.

Furthermore, optimization techniques are applied to identify the optimal nanofluid compositions and operating conditions for enhanced cooling performance. These techniques may involve conducting sensitivity analyses or employing optimization algorithms to maximize heat transfer efficiency or minimize pressure drop. The optimized parameters obtained from the simulations can guide the experimental design and provide insights for practical implementation. Additionally, economic and sustainability analyses are performed to evaluate the cost-effectiveness and environmental impact of nanofluid cooling systems. This involves assessing the production costs of nanofluids, analyzing the energy consumption and operational costs of the cooling system, and considering the long-term sustainability aspects such as nanoparticle toxicity and recyclability.

Overall, the methodology for studying nanofluid cooling for electronic components combines experimental measurements, computational simulations, optimization techniques, and economic and sustainability analyses. This integrated approach enables a comprehensive understanding of the thermal behavior of nanofluids and facilitates the development of efficient and practical cooling solutions for electronic devices.

### 3. Modeling

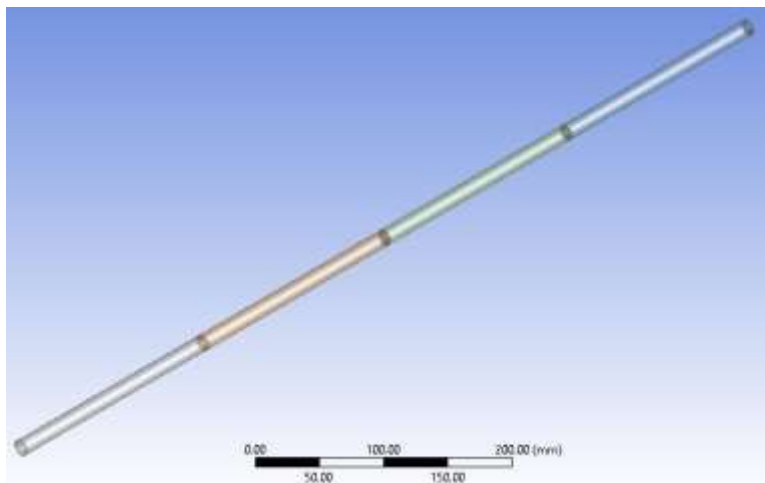


Fig. 1 3D Model of tube for 13.5 mm diameter and 800 length

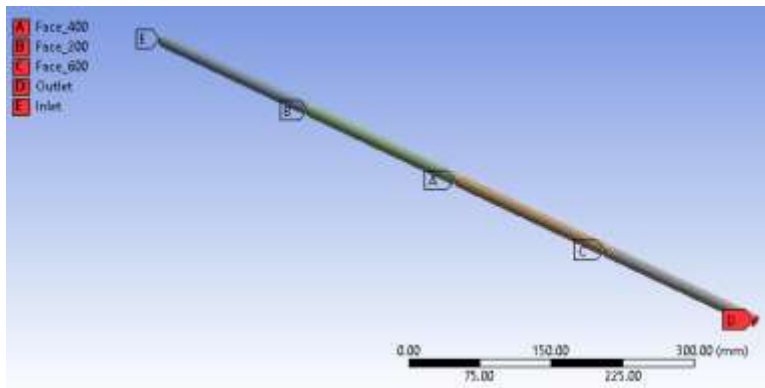
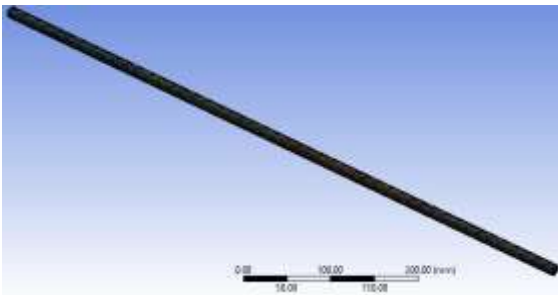
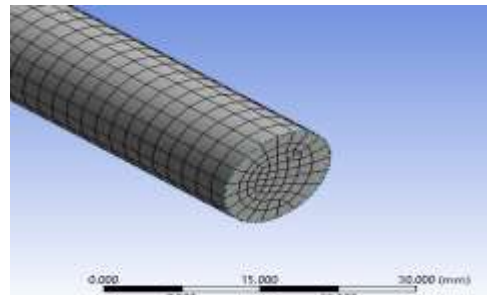


Fig. 2 Name selection to assign boundary conditions and to measure temperature at different locations

### 1. Meshing



(a) Complete meshed model



(b) Enlarged view

Fig. 3 3D meshed model for 13.5 mm diameter and 800 length

- **CFD Setting**

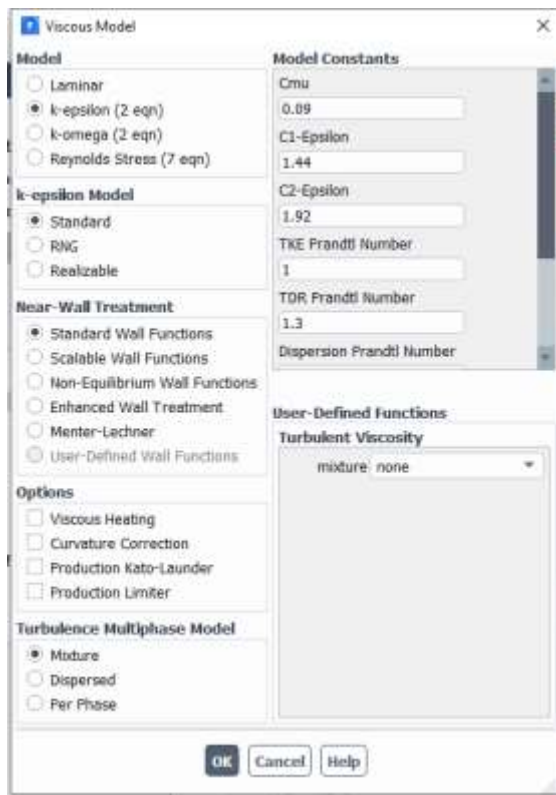


Fig. 4 k-epsilon turbulent model is selected for the analysis

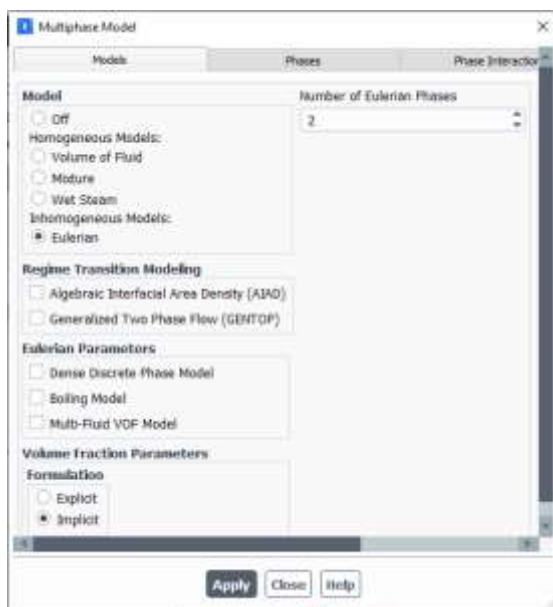


Fig. 5 Multi-Phase Eulerian model with two phases is used

- **Parameters considered for the analysis**

Various parameters are considered for the analysis of a system using CFD. The parameters are separated into two groups: the first group contains tube diameter, discharge, and Al<sub>2</sub>O<sub>3</sub> Concentration (%), while the second group contains tube diameter, discharge, and MWCNT Concentration (%). Tube Diameter has four levels of variation in the first set of parameters: 4 mm, 9 mm, and 13.5 mm. Four levels of discharge depict the system's flow rate: 4 LPM, 6 LPM, 8 LPM, and 10 LPM. Al<sub>2</sub>O<sub>3</sub> Concentration (%) represents the concentration of Al<sub>2</sub>O<sub>3</sub> nanoparticles in the nanofluid, and it has four levels: 1%, 3%, 5%, and 7%. Similarly, Tube Diameter has the same four levels of variation in the second set of parameters: 4 mm, 9 mm, and 13.5 mm. Again, there are four levels for "Discharge: 4 LPM, 6 LPM, 8 LPM, and 10 LPM. The MWCNT Concentration (%) parameter represents the percentage of MWCNT in the nanofluid, and it has four levels: 1%, 3%, 5%, and 7%. These parameters function as independent variables in the analysis, enabling a systematic examination of their effect on the performance of the system. By modifying these parameters to varying degrees, researchers can observe and analyse the corresponding changes in system behaviour, such as heat transfer efficiency, pressure decrease, and other pertinent factors.

**Table: 1 Parameters used for Al<sub>2</sub>O<sub>3</sub>**

Parameters	Level -1	Level -2	Level -3	Level -4
Tube Diameter	4 mm	9 mm	13.5 mm	-
Discharge (LPM)	4	6	8	10
Al <sub>2</sub> O <sub>3</sub> Concentration (%)	1	3	5	7

**Table: 2 Parameters used for MWCNT**

Parameters	Level -1	Level -2	Level -3	Level -4
Tube Diameter	4 mm	9 mm	13.5 mm	-
Discharge (LPM)	4	6	8	10
MWCNT Concentration (%)	1	3	5	7

**Table 3. 1 Properties of Al<sub>2</sub>O<sub>3</sub> and MWCNT Nano powders**



Properties	Al <sub>2</sub> O <sub>3</sub>	MWCNT
Diameter (nm)	20-Oct	20
Density (kg/m <sup>3</sup> )	1500	220
Sp.Heat (J/kg-K)	880	0.74
Thermal Conductivity (W/m-K)	46	3000

Different properties of Al<sub>2</sub>O<sub>3</sub> and MWCNT nanopowders are considered in analysis. In terms of diameter, Al<sub>2</sub>O<sub>3</sub> nanoparticles have a range of 10-20 nanometers, while MWCNTs have a diameter of approximately 20 nanometers. When it comes to density, Al<sub>2</sub>O<sub>3</sub> nanopowders have a higher density of 1500 kilograms per cubic meter (kg/m<sup>3</sup>) compared to MWCNTs, which have a reduced density of 220 kg/m<sup>3</sup>. This indicates that Al<sub>2</sub>O<sub>3</sub> nanopowders are more compact and have a higher mass per unit volume than MWCNTs. In terms of specific heat, Al<sub>2</sub>O<sub>3</sub> nanopowders have a higher value of 880 joules per kilogram-Kelvin (J/kg-K), indicating that they can store more heat energy per unit mass compared to MWCNTs, which have a specific heat of 0.74 J/kg-K. This implies that Al<sub>2</sub>O<sub>3</sub> nanopowders have a higher thermal capacity than MWCNTs. Regarding thermal conductivity, Al<sub>2</sub>O<sub>3</sub> nanopowders have a thermal conductivity of 46 watts per meter-Kelvin (W/m-K), while MWCNTs exhibit a significantly higher thermal conductivity of 3000 W/m-K. This indicates that MWCNTs have a much greater ability to conduct heat compared to Al<sub>2</sub>O<sub>3</sub> nanopowders. These variations in properties can influence the behavior and efficacy of these nanoparticles in various applications, such as thermal transfer, electronics, or materials science.

### Calculations for CFD:

#### For D= 4 mm

$$Q = \rho A V$$

$$Q = 4 \text{ LPM}$$

$$= \frac{4}{10^3 \times 60} \text{ m}^3/\text{s}$$

$$\frac{4}{10^3 \times 60} = 1000 \times \frac{\pi}{4} \times V$$

$$V = \frac{4 \times 4}{60 \times 1000 \times 1000 \times \pi \times (4 \times 10^{-3})^2} = \frac{16}{10^6 \times \pi \times (4 \times 10^{-3})^2}$$

$$V = \frac{16}{60 \times 10^6 \times \pi \times 16 \times 10^{-6}} = \frac{16}{60 \times 16 \times \pi} = \frac{1}{60 \pi} = 0.0053 \text{ m/s}$$

$$Q = 6 \text{ LPM} = \frac{6 \times 10^{-3}}{60} = \text{m}^3/\text{s}$$

$$\frac{6 \times 10^{-3}}{60} = 1000 \times \frac{\pi}{4} \times ((0.004)^2) \times V$$

$$V = \frac{6 \times 10}{60 \times 10} \times \frac{4}{\pi \times 10^{-4}}$$

$$V = \frac{6 \times 4}{60 \times 1000 \times 1000 \pi \times (4 \times 10^{-3})}$$

$$= \frac{6 \times 4}{60 \times \pi \times 16} = \frac{6 \times 4}{60 \times \pi \times 16} = 6 \times 0.00132$$

$$= 0.007961 \text{ m/s}$$

$$Q = 8 \text{ LPM} \quad V = 8 \times 0.007961 \quad V = 0.59688 \text{ m/s}$$

$$Q = 10 \text{ LPM} \quad V = 10 \times 0.007961 = 0.7961 \text{ m/s}$$

**For D = 9mm**

$$Q = 4 \text{ LPM}$$

$$= \frac{4 \times 10}{60} = \text{m/s}$$

$$= \frac{4}{10^3 \times 60} = 1000 \times \frac{4}{4} (6.00)^2 \times V$$

$$V = \frac{4 \times 4}{10^3 \times 60 \times 10^3 \times 8 \times 10^{-6}}$$

$$= \frac{4 \times 4}{60 \times 8 \times 481}$$

$$V = V = 0.00104 \text{ m/s}$$

$$Q = 6 \text{ LPM}$$

$$V = 6 \times 0.0002621 = 0.0015722 \text{ m/s}$$

$$Q = 8 \text{ LPM}$$

$$V = 0.002096 \text{ m/s}$$

$$Q = 10 \text{ LPM}$$

$$V = 0.002621 \text{ m/s}$$

**For D = 13.5mm**

$$Q = 4 \text{ LPM}$$

$$x = \frac{4}{100 \times 60} = 100 \times \frac{\pi (13.5 \times 10^{-3})^2}{4} \times V$$

$$V_s = 4 \frac{4}{10^3 \times 10^3 \times 60 \times \pi \times (13.5 \times 10^{-3})}$$

$$= 4 \frac{4}{60 \times \pi \times 13.5^2} = \frac{4 \times 4}{34335.4}$$

$$= 4 \times 0.00011649$$

$$V = 0.0004659 \text{ m/s}$$

$$Q = 6\text{LPM} \quad V = 0.00069897 \text{ m/s}$$

$$Q = 8\text{LPM} \quad V = 0.00093196 \text{ m/s}$$

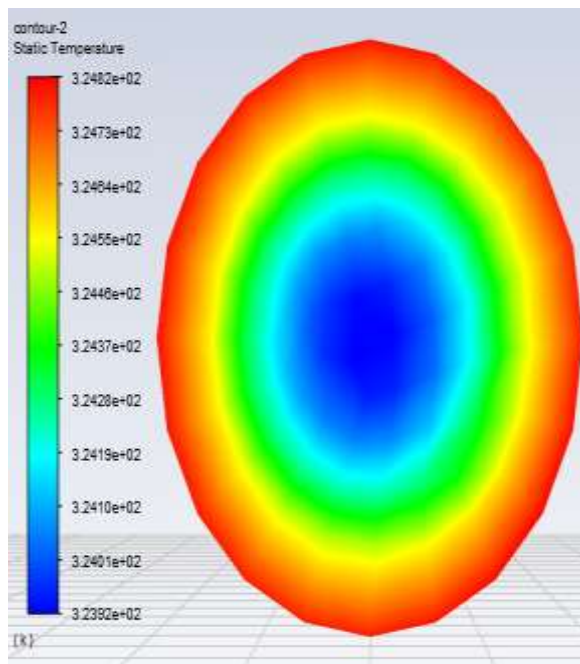
$$Q = 10\text{LPM} \quad V = 0.0011649 \text{ m/s}$$

#### 4. Result and discussion

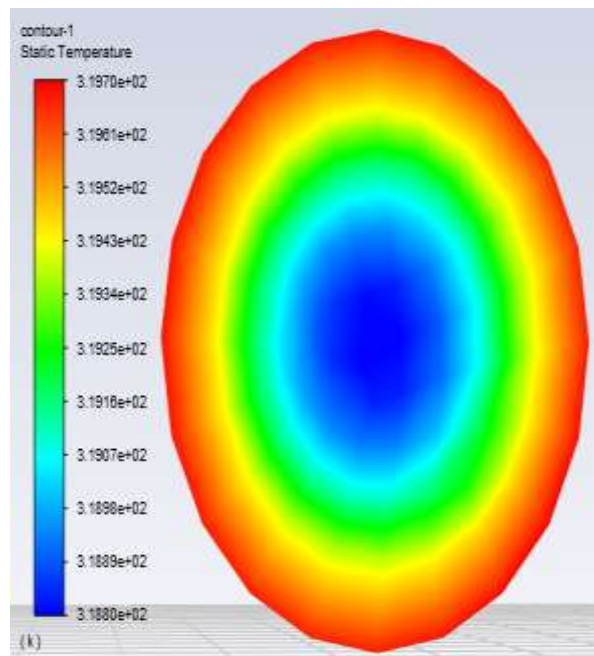
Using different parameters, CFD analysis is done. For water with diameters of 4, 9, and 13.5 mm at 4, 6, 8, and 10 LPM. Also, identical studies were done for 0.7% Al<sub>2</sub>O<sub>3</sub> and MWCNT with water. Results show the Temperature Distribution of water containing 0.7% Al<sub>2</sub>O<sub>3</sub> and water containing 0.7% MWCNT at the Outlet of a Tube with a variable diameter and discharge rate.

#### ❖ temperature distribution of Water Exiting a Tube with a Discharge of 4, 6, 8 and 10 LMP

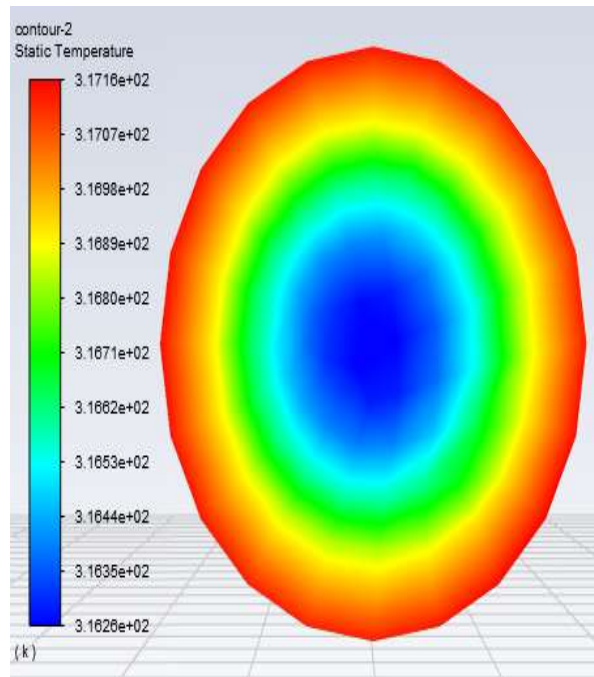
##### Tube Diameter = 4 mm



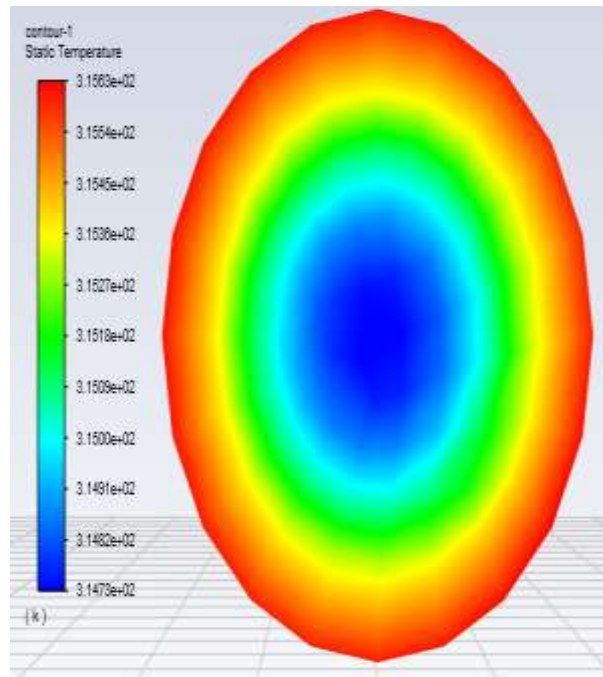
**Fig: 6 Discharge of 4 LMP**



**Fig: 7 Discharge of 6 LMP.**



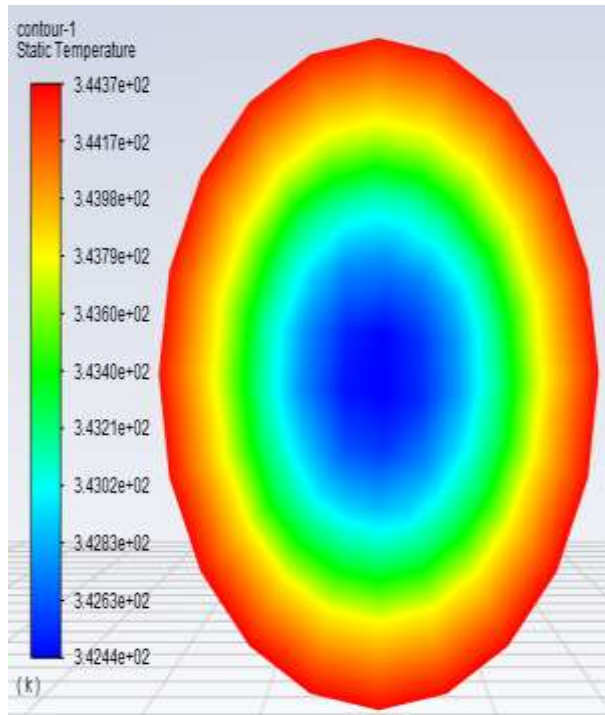
**Fig: 8 Discharge of 8 LMP**



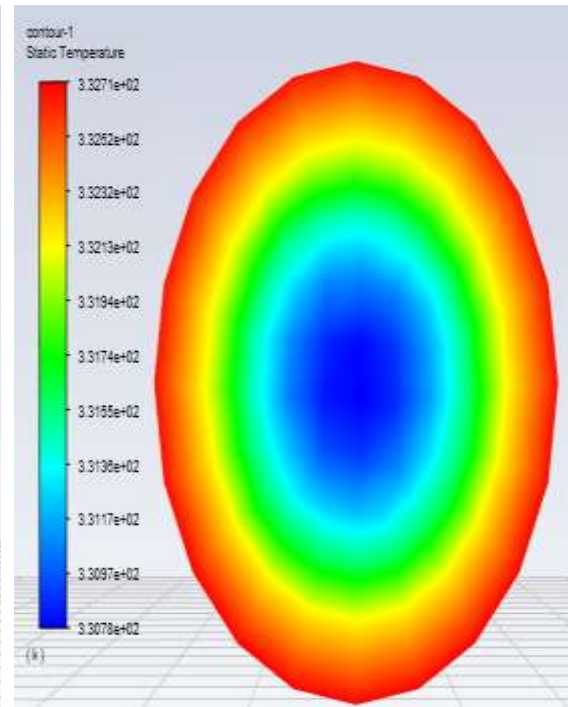
**Fig: 9 Discharge of 10 LMP**

The conducted CFD analysis in ANSYS software provided insightful results for the cooling of electronic components using water as the base fluid. The contours for static temperature offer valuable information about the thermal behavior within the system. The tube diameter of 4 mm and a discharge rate of 4 LMP (Liters per Minute) were considered for the analysis. The minimum and maximum values of the static temperature observed in the system were found to be  $3.2392e+02$  and  $3.2482e+02$ , respectively. These temperature values represent the thermal distribution within the cooling system. The minimum temperature value of  $3.2392e+02$  indicates areas of relatively lower temperature, where effective heat dissipation is occurring. On the other hand, the maximum temperature value of  $3.2482e+02$  corresponds to areas of higher temperature, potentially indicating regions where heat transfer may be less efficient. The flow rate or discharge of water through the tube was set at 6 LPM. The contour plots generated from the analysis represent the distribution of static temperature within the system. The minimum and maximum values of the temperature observed in the analysis are  $3.1880e+02$  and  $3.1970e+02$ , respectively. The results of the CFD analysis conducted for water as the cooling fluid, with a tube diameter of 4 mm and a discharge rate of 8 LPM, revealed the distribution of static temperature within the system. The contours obtained from the analysis provide valuable insights into the thermal behavior of the electronic component cooling process. The minimum and maximum values of the static temperature observed in the system are  $3.1626e+02$  and  $3.1716e+02$ , respectively. These values represent the temperature range experienced by the electronic component during the cooling process. The analysis considered a tube diameter of 4 mm and a discharge rate of 10 LMP (Liters per Minute). The results of the analysis revealed the distribution of static temperature within the system. The minimum temperature recorded was  $3.1473e+02$  while the maximum temperature observed was  $3.1563e+02$ .

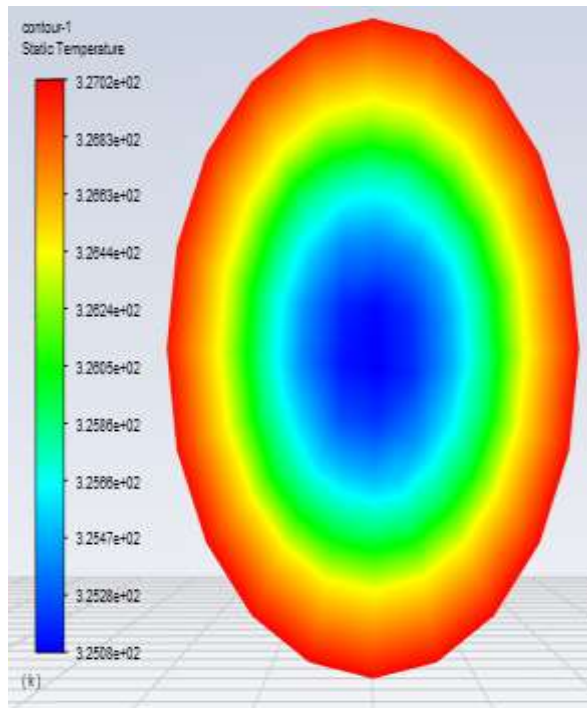
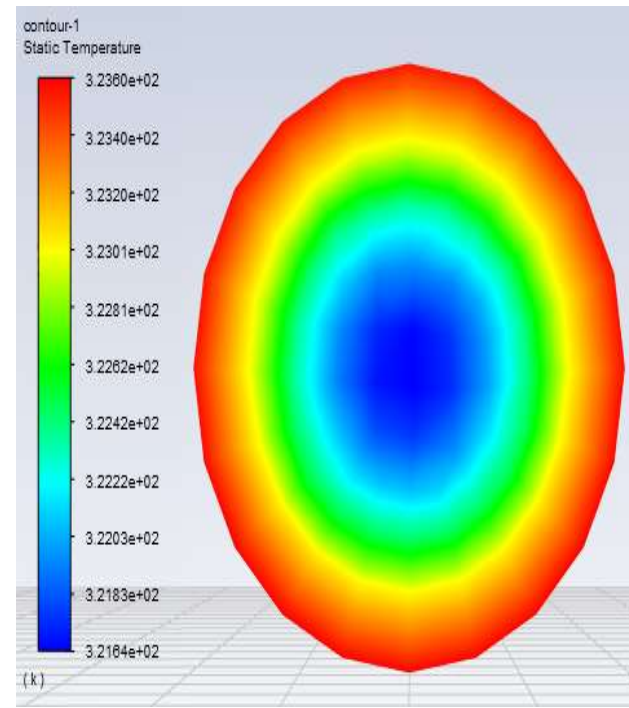
**Tube Diameter = 9 mm**



**Fig: 10 Discharge of 4 LMP**



**Fig: 11 Discharge of 6 LMP**

**Fig: 12 Discharge of 8 LMP****Fig: 13 Discharge of 10 LMP**

For a fixed tube diameter of 9 mm, the results illustrate the static temperature distribution at the outlet for discharge rates of 4 LMP, 6 LMP, 8 LMP, and 10 LMP. In the case of a discharge rate of 4 LMP, the minimum and maximum static temperature values at the outlet are  $3.4244e+02$  and  $3.4437e+02$ , respectively. These values indicate the temperature range experienced by the water as it exits the cooling system. Similarly, for a discharge rate of 6 LMP, the temperature contours display the static temperature distribution at the outlet. The minimum and maximum temperature values are  $3.3078e+02$  and  $3.3271e+02$ , respectively. For a discharge rate of 8 LMP, the temperature contours continue to illustrate the static temperature distribution. The minimum temperature recorded at the outlet is  $3.2508e+02$ , while the maximum temperature reaches  $3.2702e+02$ . Lastly, with a discharge rate of 10 LMP, the temperature contours depict the static temperature distribution at the outlet. The minimum temperature value is  $3.2164e+02$ , and the maximum temperature value is  $3.2360e+02$ . These results provide valuable insights into the thermal behavior of the water within the cooling system under different operating conditions. By visualizing the temperature contours, it becomes possible to identify regions of higher and lower temperatures at the outlet. This analysis allows for an evaluation of the cooling system's effectiveness and the assessment of the water's thermal performance as a cooling medium for electronic components.

**Tube Diameter = 13.5 mm**

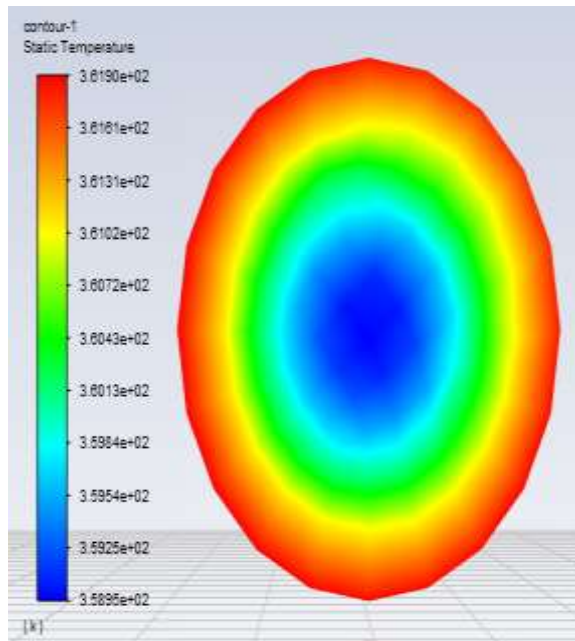


Fig: 14 Discharge of 4 LMP

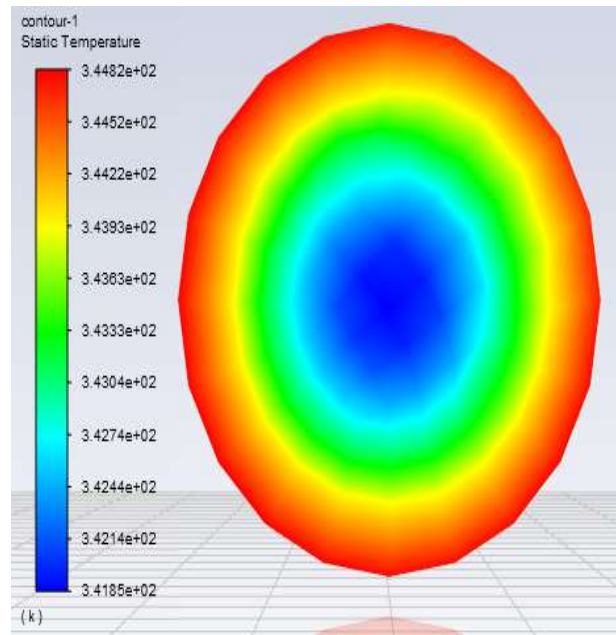


Fig: 15 Discharge of 6 LMP

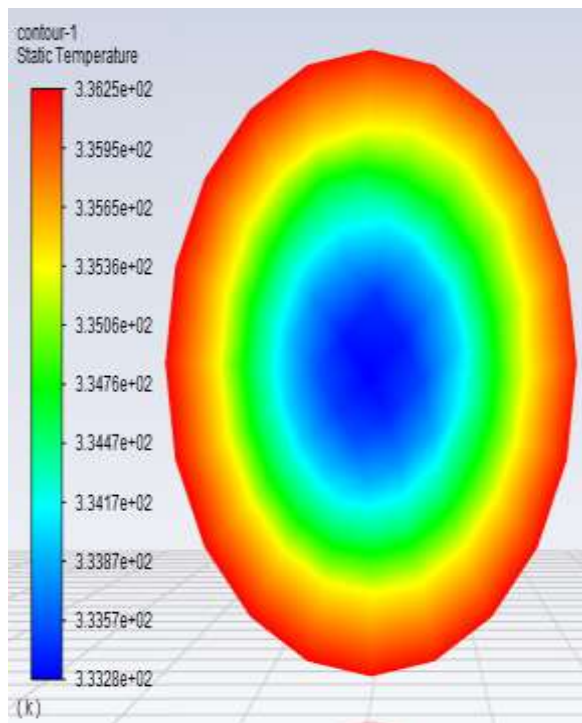


Fig: 16 Discharge of 8 LMP

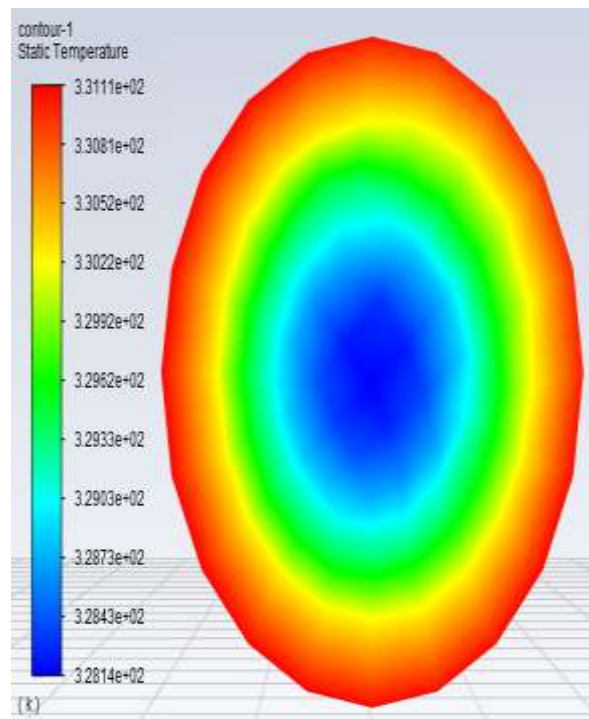
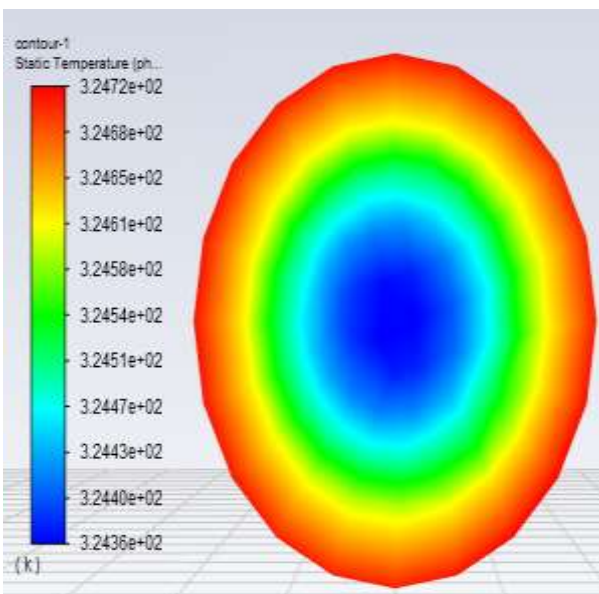


Fig: 17 Discharge of 10 LMP

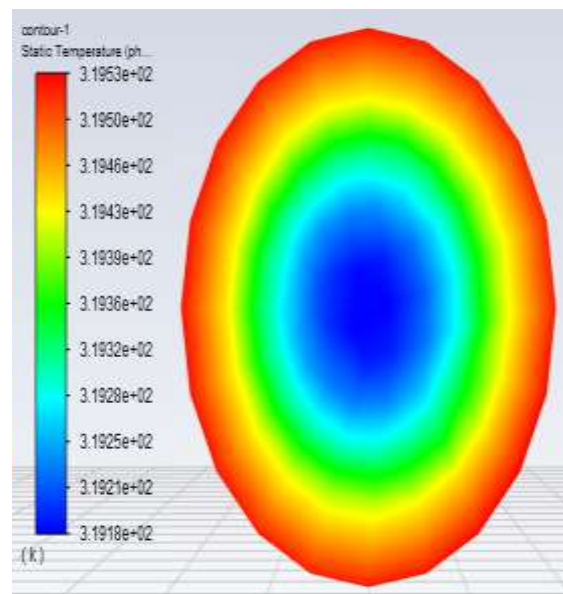
The results focus on the outlet temperature contours for a tube diameter of 13.5 mm and different discharge rates (LMP). The obtained minimum and maximum temperature values for each scenario are summarized as follows: For a discharge rate of 4 LMP, the temperature contours indicate that the minimum temperature recorded at the outlet is  $3.5895e+02$ , while the maximum temperature reaches  $3.6190e+02$ . With a discharge rate of 6 LMP, the temperature contour analysis reveals a slightly lower temperature profile compared to the previous scenario. The minimum temperature recorded at the outlet is  $3.4185e+02$ , while the maximum temperature reaches  $3.4482e+02$ . This indicates that increasing the discharge rate leads to a decrease in temperature, suggesting improved heat dissipation capabilities. Moving on to a discharge rate of 8 LMP, the temperature contour plots show a further reduction in temperature. The minimum temperature at the outlet is measured as  $3.3328e+02$ , while the maximum temperature reaches  $3.3625e+02$ . This trend indicates that increasing the fluid flow rate enhances the cooling efficiency, resulting in lower temperatures. Finally, for a discharge rate of 10 LMP, the temperature contour analysis demonstrates a continued decrease in temperature. The minimum temperature at the outlet is  $3.2814e+02$ , and the maximum temperature is  $3.3111e+02$ . These values indicate the further cooling effect achieved by increasing the fluid discharge rate.

❖ **Temperature Distribution of Water Containing 0.7% Al<sub>2</sub>O<sub>3</sub> at the Outlet of a Tube with a Discharge of 4, 6, 8 and 10 LMP**

**Tube Diameter = 4 mm**

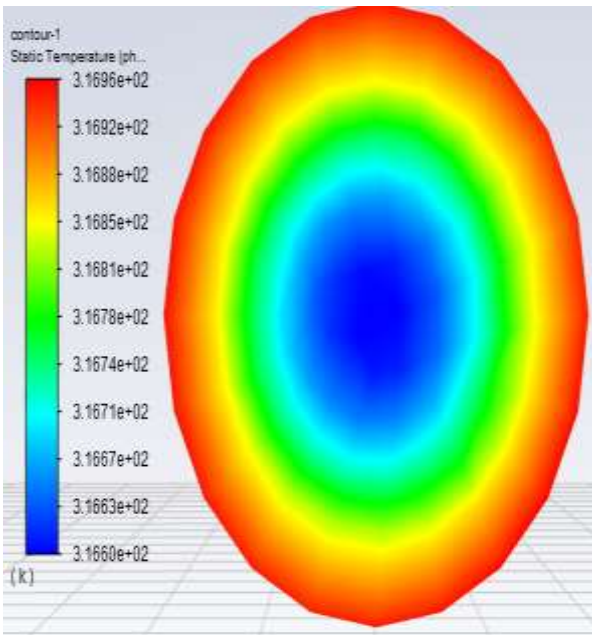
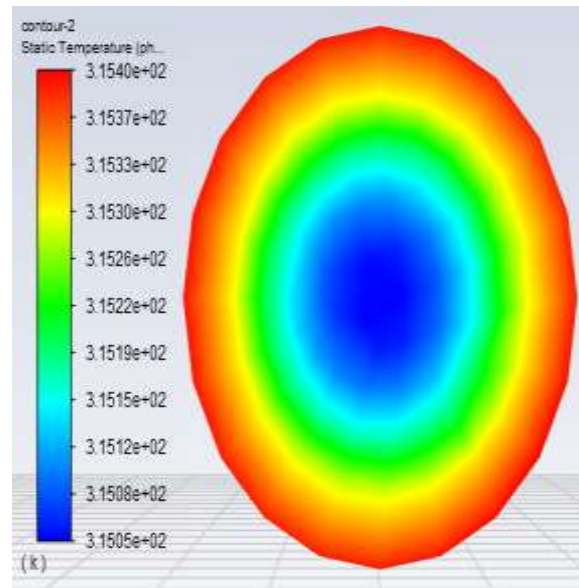


**Fig: 18 Discharge of 4 LMP**



**Fig: 19 Discharge of 6 LMP**



**Fig: 20 Discharge of 8 LMP****Fig: 21 Discharge of 10 LMP**

The conducted CFD analysis insights into the temperature distribution of water containing 0.7% Al<sub>2</sub>O<sub>3</sub> nanoparticles at different operating conditions. The results focus on the outlet temperature contours for a tube diameter of 4 mm and various discharge rates (LMP). For a discharge rate of 4 LMP, the temperature contour indicates that the minimum and maximum values of temperature are approximately 324.72 K and 324.36 K, respectively. This suggests that the addition of 0.7% Al<sub>2</sub>O<sub>3</sub> nanoparticles to water slightly reduces the overall temperature, enhancing the cooling effect at this operating condition. At a discharge rate of 6 LMP, the temperature contour demonstrates a similar trend, with the minimum and maximum temperature values measuring around 319.53 K and 319.18 K, respectively. These results indicate a further reduction in temperature compared to the previous scenario, indicating that the presence of nanoparticles continues to enhance the cooling capability. Increasing the discharge rate to 8 LMP results in a temperature contour where the minimum and maximum temperature values are approximately 316.96 K and 316.60 K, respectively. The trend of temperature reduction with the inclusion of nanoparticles persists, highlighting the improved heat dissipation capabilities of the nanofluid. Finally, at a discharge rate of 10 LMP, the temperature contour shows a further decrease in temperature. The minimum and maximum temperature values are approximately 315.40 K and 315.05 K, respectively. These results reaffirm the effectiveness of the nanofluid in enhancing the cooling process and maintaining lower temperatures at higher flow rates. Overall, the CFD analysis demonstrates that the addition of 0.7% Al<sub>2</sub>O<sub>3</sub> nanoparticles to water has a positive impact on heat transfer and cooling efficiency. The temperature contours clearly depict the reduction in temperature at the outlet of the system as the discharge rate increases, indicating the potential of nanofluids for effectively dissipating heat in electronic components cooling applications.

**Tube Diameter = 9 mm**

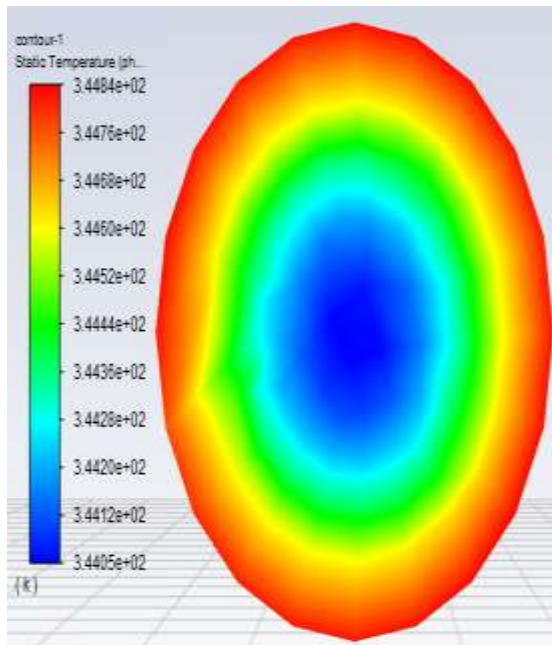


Fig: 22 Discharge of 4 LMP

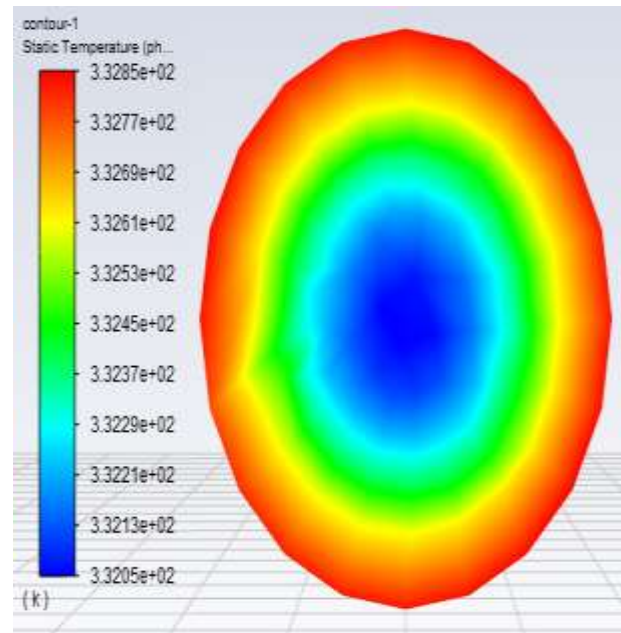


Fig: 23 Discharge of 6 LMP

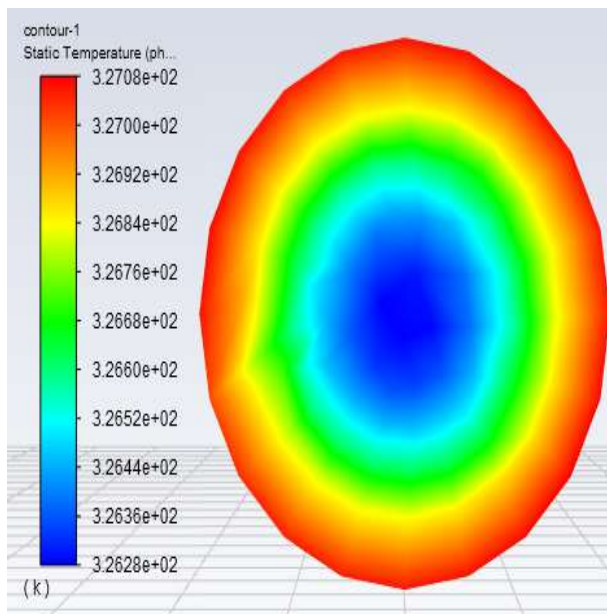


Fig: 24 Discharge of 8 LMP

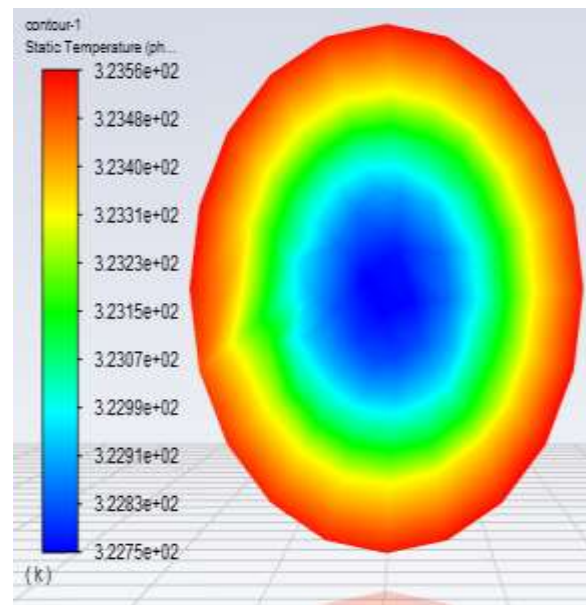
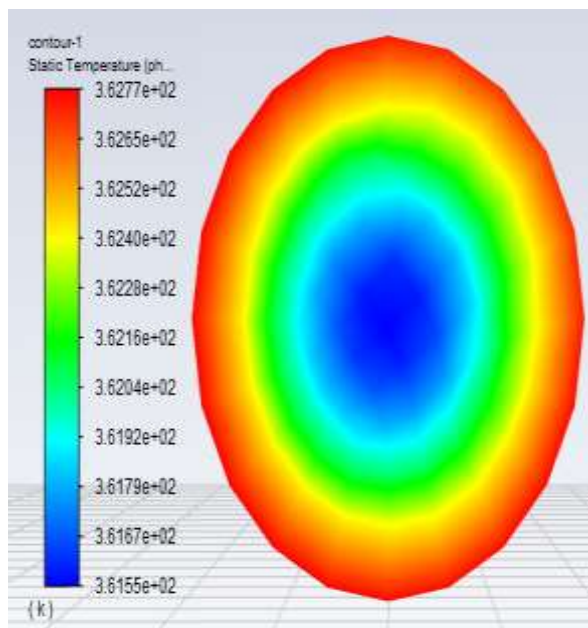


Fig: 25 Discharge of 10 LMP

The conducted CFD analysis software presents the temperature contours for water with 0.7% Al<sub>2</sub>O<sub>3</sub> (alumina) nanoparticles at the outlet of a cooling system. The analysis focused on a tube diameter of 9 mm

and different discharge rates, namely 4 LMP, 6 LMP, 8 LMP, and 10 LMP. For the case of a tube diameter of 9 mm and a discharge rate of 4 LMP, the temperature contours show a range of values. The minimum temperature recorded is  $3.4484e+02$ , while the maximum temperature reached is  $3.4405e+02$ . These contours represent the temperature distribution at the outlet of the cooling system, indicating how the heat is dissipated when using water with 0.7%  $Al_2O_3$  nanoparticles. Similarly, for a discharge rate of 6 LMP, the temperature contours exhibit a different range of values. The minimum temperature observed is  $3.3285e+02$ , while the maximum temperature recorded is  $3.3205e+02$ . These contours demonstrate the thermal behavior of the cooling system under this specific operating condition. Continuing with a discharge rate of 8 LMP, the temperature contours showcase another set of values. The minimum temperature registered is  $3.2708e+02$ , whereas the maximum temperature attained is  $3.2628e+02$ . These contours provide insights into the temperature distribution when water with 0.7%  $Al_2O_3$  nanoparticles is utilized in the cooling system with the specified discharge rate. Lastly, for a discharge rate of 10 LMP, the temperature contours depict a different range of values. The minimum temperature observed is  $3.2356e+02$ , while the maximum temperature reached is  $3.2275e+02$ . These contours offer an understanding of the thermal characteristics at the outlet when using water with 0.7%  $Al_2O_3$  nanoparticles in the cooling system with the given discharge rate.

### Tube Diameter = 13.5 mm



**Fig: 26 Discharge of 4 LMP**

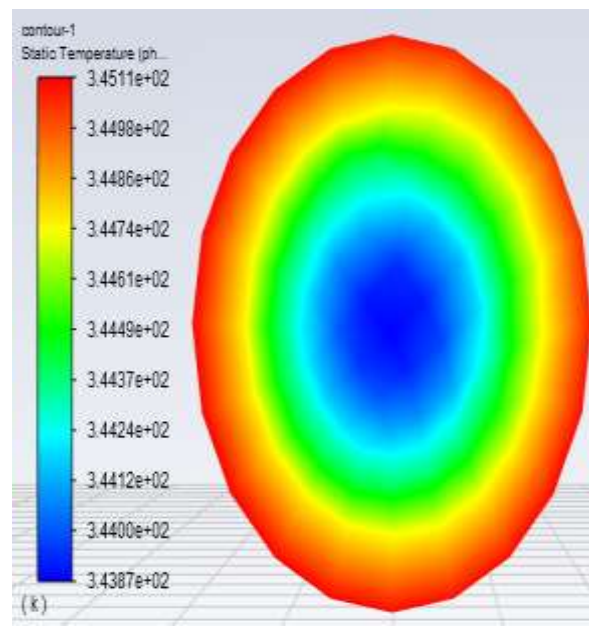


**Fig: 27 Discharge of 6 LMP**

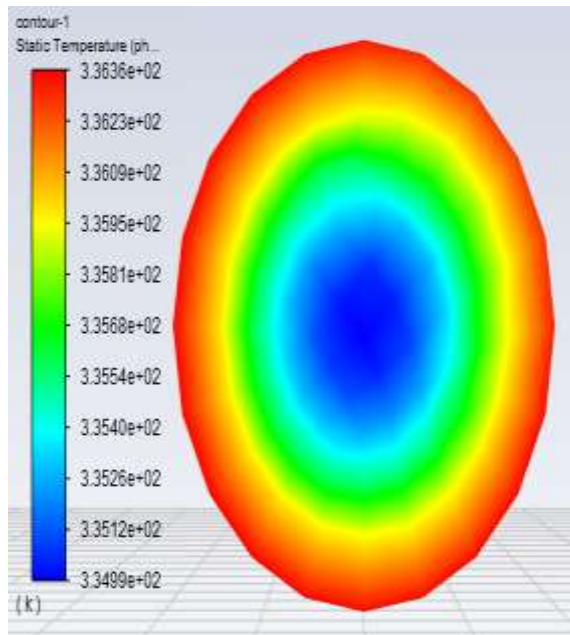


Fig: 28 Discharge of 8 LMP

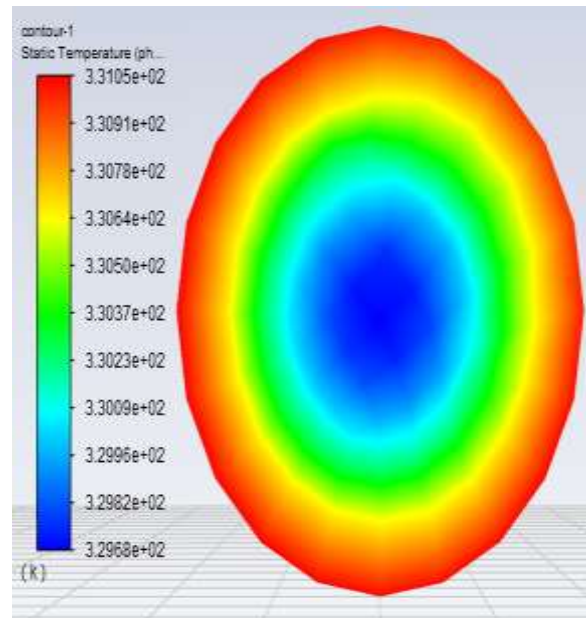


Fig: 29 Discharge of 10 LMP

The results of the CFD analysis valuable insights into the temperature distribution within the cooling system when water is used as the base fluid with a 0.7% Al<sub>2</sub>O<sub>3</sub> nanoparticle concentration. The contours of static temperature at the outlet for various operating conditions were examined, specifically for a tube diameter of 13.5 mm. For a discharge rate of 4 LMP (Liters per Minute), the temperature contour indicates that the minimum and maximum temperature values observed are 3.6277e+02 and 3.6155e+02, respectively. This suggests that the cooling system effectively dissipates heat, maintaining a relatively uniform temperature profile at the outlet. When the discharge rate is increased to 6 LMP, the temperature contour shows a slightly lower temperature distribution. The minimum and maximum temperature values recorded are 3.4511e+02 and 3.4387e+02, respectively. This indicates that the higher flow rate enhances the cooling performance, resulting in a reduction in temperature. Further increasing the discharge rate to 8 LMP leads to a continued improvement in the cooling efficiency. The temperature contour reveals a lower temperature profile compared to the previous cases. The minimum and maximum temperature values obtained are 3.3636e+02 and 3.3499e+02, respectively, indicating a more effective heat dissipation. Finally, for a discharge rate of 10 LMP, the temperature contour demonstrates a further decrease in temperature throughout the system. The minimum and maximum temperature values observed are 3.3105e+02 and 3.2968e+02, respectively. This suggests that the cooling system operates at an even lower temperature, indicating enhanced heat transfer performance. Overall, the CFD analysis results illustrate the effect of varying discharge rates on the temperature distribution within the cooling system. As the discharge rate increases, the system exhibits improved heat dissipation capabilities, resulting in lower temperatures at the outlet.

#### ❖ Temperature Distribution of Water Containing 0.7% MWCNT at the Outlet of a Tube with a Discharge of 4, 6, 8 and 10 LMP

**Tube Diameter = 4 mm**

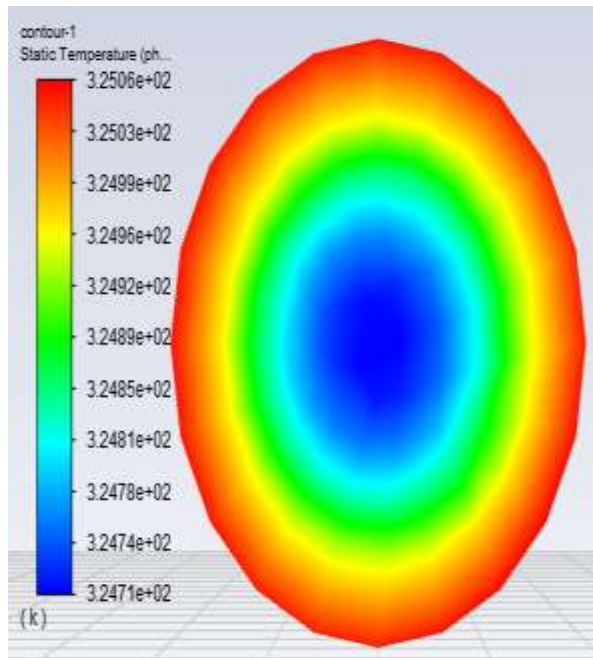


Fig: 30 Discharge of 4 LMP

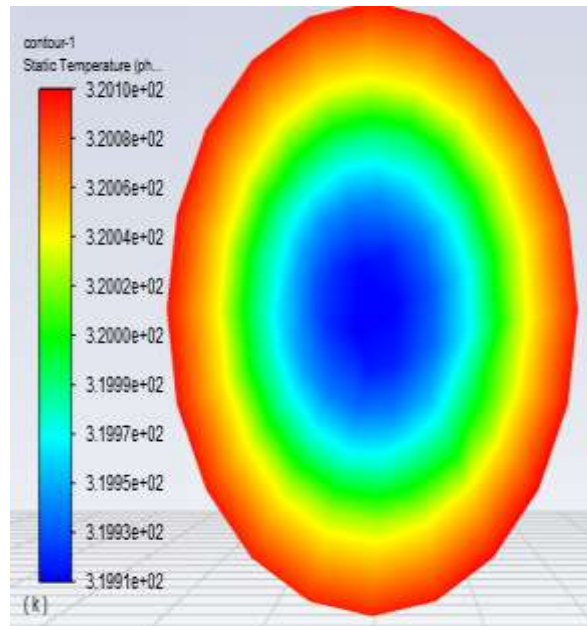


Fig: 31 Discharge of 6 LMP

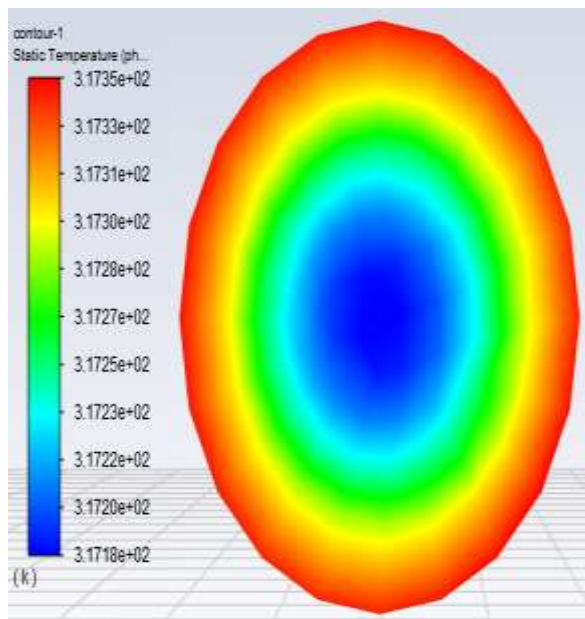


Fig: 32 Discharge of 8 LMP

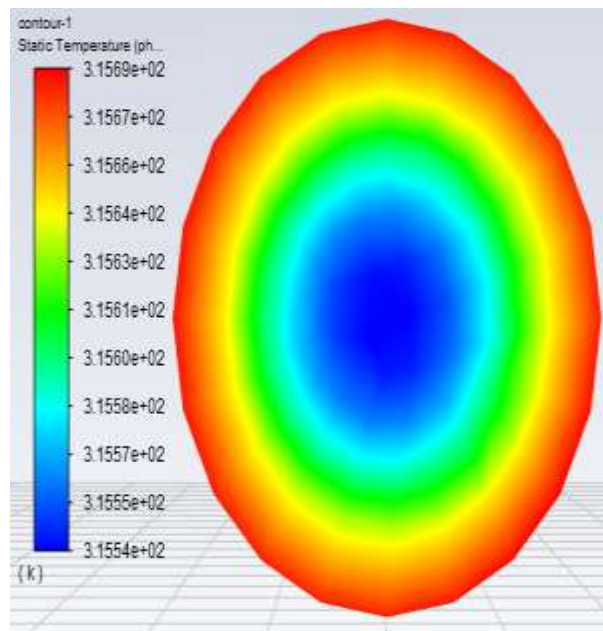
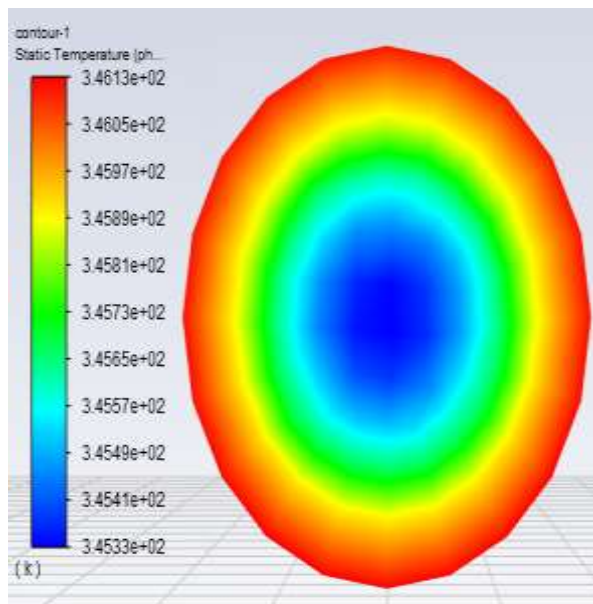


Fig: 33 Discharge of 10 LMP

The temperature contours obtained at the outlet for different combinations of tube diameter and discharge rates reveal interesting findings. For a tube diameter of 4mm and a discharge rate of 4 LMP (Liters per Minute), the temperature contour of water with 0.7% MWCNT shows a maximum temperature of  $3.2506 \times 10^2$  and a minimum temperature of  $3.2471 \times 10^2$ . These values indicate a relatively small temperature difference, suggesting that the heat transfer enhancement with the given parameters may be limited. When the discharge rate is increased to 6 LMP, the temperature contour shows a slightly lower maximum temperature of  $3.2010 \times 10^2$  and a minimum temperature of  $3.1991 \times 10^2$ . Although the temperature values are slightly reduced compared to the previous case, the difference is still relatively small. This indicates that increasing the discharge rate does not significantly improve the heat transfer performance with the chosen tube diameter and MWCNT concentration. Further analysis with a discharge rate of 8 LMP shows a temperature contour with a maximum temperature of  $3.1735 \times 10^2$  and a minimum temperature of  $3.1718 \times 10^2$ . These values suggest a gradual decrease in temperature, indicating a slight improvement in heat transfer efficiency compared to the previous cases. Lastly, when the discharge rate is set at 10 LMP, the temperature contour exhibits a maximum temperature of  $3.1569 \times 10^2$  and a minimum temperature of  $3.1554 \times 10^2$ . These values demonstrate a further reduction in temperature, indicating improved heat dissipation compared to the earlier cases. Overall, the temperature contours highlight the influence of the discharge rate on heat transfer enhancement using MWCNT-infused water. The results suggest that increasing the discharge rate leads to a gradual improvement in heat dissipation, resulting in lower temperatures at the outlet.

### Tube Diameter = 9 mm



**Fig: 34 Discharge of 4 LMP**

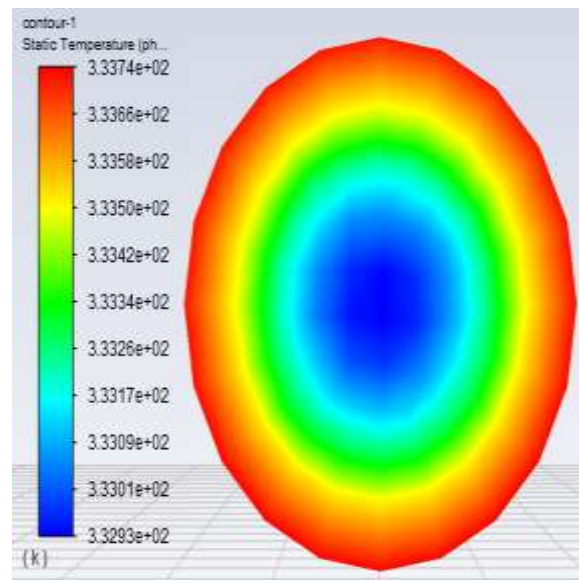


**Fig: 35 Discharge of 6 LMP**

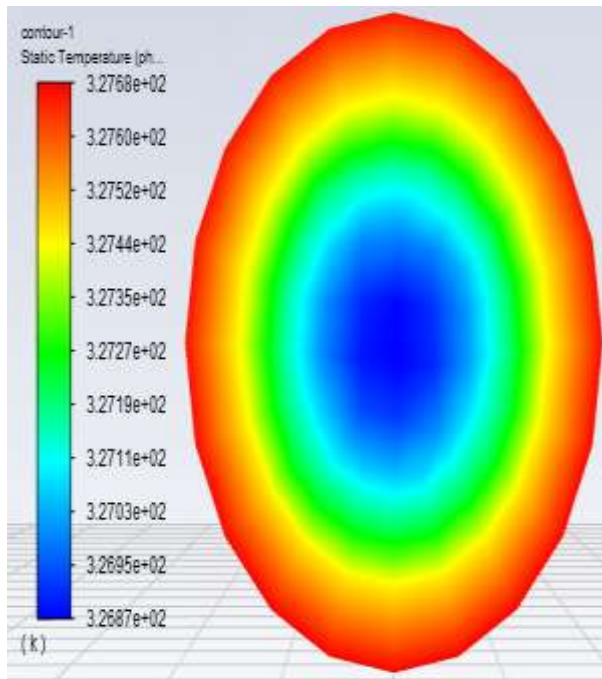


**Fig: 36 Discharge of 8 LMP**

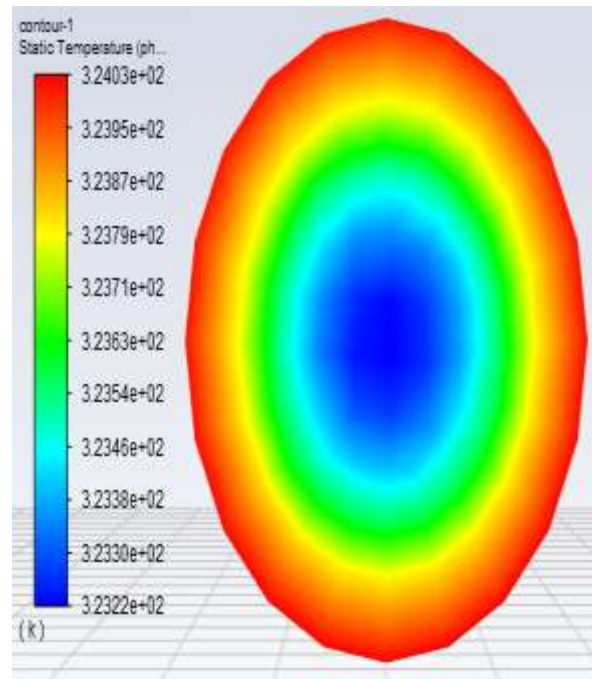


**Fig: 37 Discharge of 10 LPM**

The conducted CFD analysis provides temperature contours for the cooling system using water with 0.7% Multi-Walled Carbon Nanotubes (MWCNT) as a nanofluid. The analysis focuses on the outlet temperature at different operating conditions, considering a tube diameter of 9 mm and varying discharge rates. For a discharge rate of 4 LMP (Liters per Minute), the temperature contour shows a range of values from  $3.4533e+02$  to  $3.4613e+02$ . This indicates that the cooling system effectively dissipates heat, resulting in a relatively uniform temperature distribution at the outlet. When the discharge rate is increased to 6 LMP, the temperature contour exhibits a slightly lower range of values, ranging from  $3.3293e+02$  to  $3.3374e+02$ . This suggests that the cooling efficiency is maintained even with a higher flow rate, indicating the effectiveness of the nanofluid in enhancing heat transfer. At a discharge rate of 8 LMP, the temperature contour reveals a further decrease in the temperature range, ranging from  $3.2687e+02$  to  $3.2768e+02$ . This indicates that the cooling system is successfully dissipating more heat, resulting in lower temperatures at the outlet. Finally, for a discharge rate of 10 LMP, the temperature contour demonstrates the lowest range of values among the considered cases, ranging from  $3.2322e+02$  to  $3.2403e+02$ . This suggests that the cooling system achieves its highest level of heat dissipation and effectively lowers the temperature of the electronic components. Overall, the temperature contours obtained from the CFD analysis illustrate the effectiveness of using water with 0.7% MWCNT as a nanofluid in enhancing heat transfer and cooling electronic components. The decreasing temperature range with increasing discharge rates signifies the improved cooling performance of the system, highlighting the potential of nanofluids for heat transfer enhancement in electronic cooling applications.

**Tube Diameter = 13.5 mm**

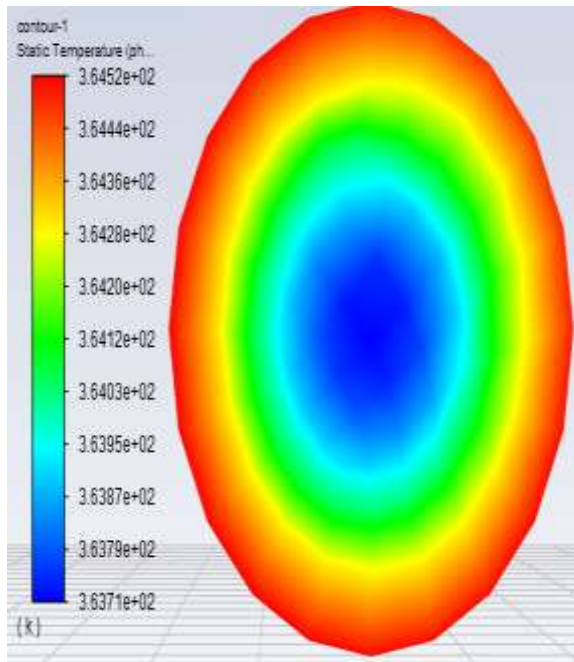


Fig: 38 Discharge of 4 LMP

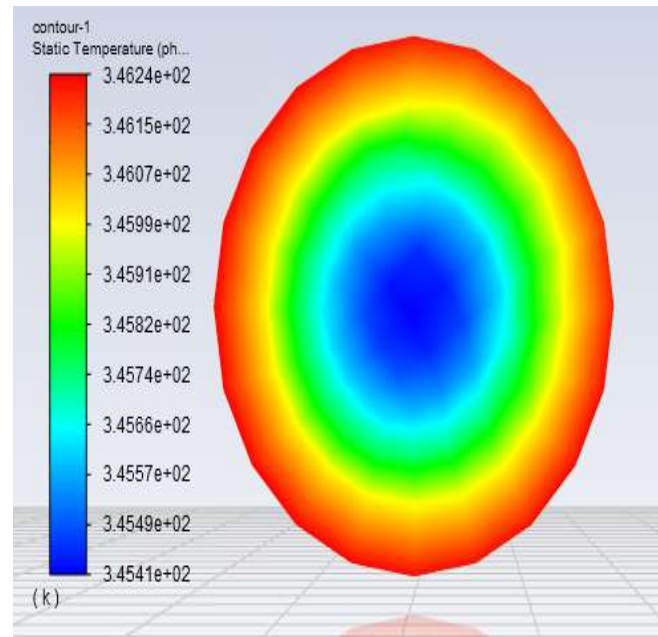


Fig: 39 Discharge of 6 LMP

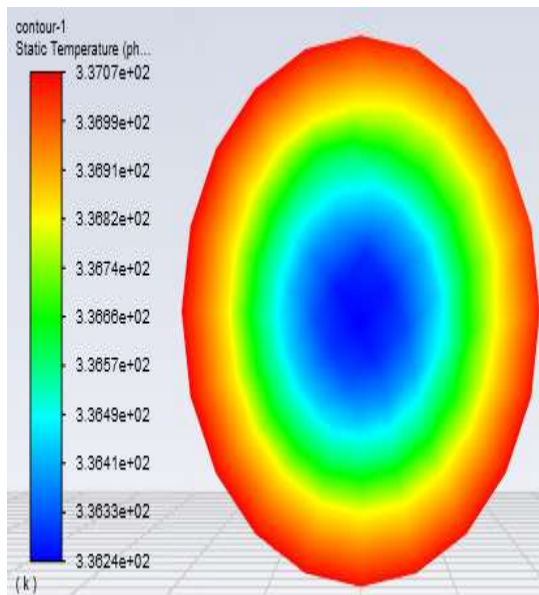


Fig: 40 Discharge of 8 LMP

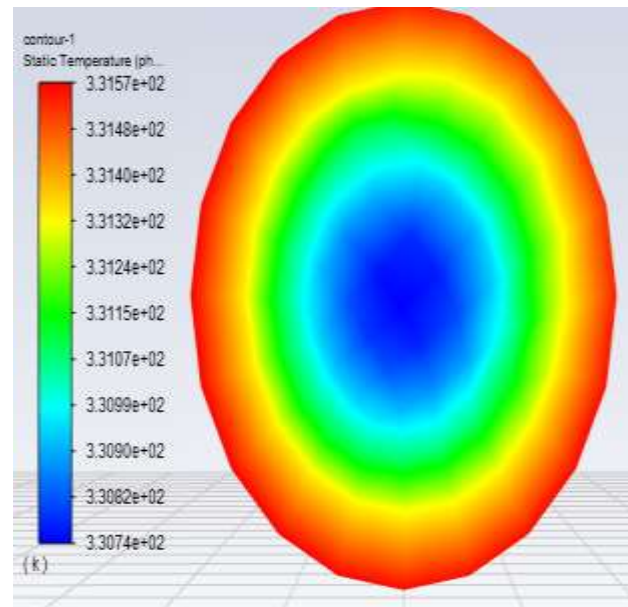


Fig: 41 Discharge of 10 LMP



The conducted CFD analysis insights into the temperature distribution for water with 0.7% MWCNT (multi-walled carbon nanotube) at the outlet of a cooling system. The analysis considers different operating conditions, specifically tube diameter and discharge rates, to evaluate the impact on the temperature contours. For a tube diameter of 13.5 mm and a discharge rate of 4 LMP (liters per minute), the temperature contour reveals a range of temperatures. The minimum temperature observed is  $3.6371e+02$  (in Kelvin) while the maximum temperature is  $3.6452e+02$ . These results depict the thermal behavior of the nanofluid as it flows through the cooling system under these specific conditions. Similarly, when the discharge rate is increased to 6 LMP, the temperature contour for the same tube diameter shows a different distribution. The minimum temperature at the outlet is  $3.4541e+02$ , while the maximum temperature reaches  $3.4624e+02$ . This variation in temperature demonstrates the influence of the increased flow rate on heat dissipation. Furthermore, for a discharge rate of 8 LMP, the temperature contour presents a further shift in the thermal distribution. The minimum temperature at the outlet is  $3.3624e+02$ , while the maximum temperature reaches  $3.3707e+02$ . These results indicate how altering the operating conditions can affect the temperature profile within the cooling system. Lastly, when the discharge rate is increased to 10 LMP, the temperature contour shows another set of temperature values. The minimum temperature recorded is  $3.3074e+02$ , while the maximum temperature is  $3.3157e+02$ . These findings illustrate the changes in the cooling efficiency at different flow rates. Overall, the CFD analysis highlights the impact of varying tube diameter and discharge rates on the temperature distribution of the nanofluid at the outlet of the cooling system. The obtained results provide valuable information for optimizing the cooling performance and designing efficient electronic component cooling systems that utilize nanofluids with MWCNT additives.

## 5. Conclusion

In this study, CFD analysis was conducted using ANSYS software to investigate the thermal behavior of a cooling system for electronic components. The focus of the analysis was on the use of water and water-based nanofluids as the cooling medium. The results of the CFD analysis provided valuable insights into the temperature distribution within the cooling system under different operating conditions. The analysis considered various factors such as tube diameter and discharge rates to assess their impact on heat transfer and cooling efficiency. When water was used as the base fluid, the temperature contours at the outlet of the cooling system showed the thermal behavior of the electronic components. The minimum and maximum temperature values observed varied depending on the tube diameter and discharge rate. These temperature values provided information about areas of effective heat dissipation and regions where heat transfer may be less efficient. Furthermore, the study explored the use of nanofluids, specifically water with 0.7%  $Al_2O_3$  nanoparticles and water with 0.7% MWCNT nanoparticles, for heat transfer enhancement. The temperature contours obtained for these nanofluids at different operating conditions demonstrated their effect on cooling performance. The addition of nanoparticles resulted in a reduction in temperature, indicating improved heat dissipation capabilities. Overall, the CFD analysis presented in this study provides valuable insights into the thermal behavior and heat transfer enhancement of a cooling system for electronic components. The temperature contours obtained through the analysis enable the evaluation of cooling system effectiveness and the assessment of different cooling mediums, including nanofluids, for efficient heat dissipation in electronic component cooling applications.

The future scope of nanofluid cooling research for electronic components includes multiple areas of investigation. First, experimental validation is required to validate the results obtained from computational simulations. The optimization of nanofluid composition, including the variation of nanoparticle concentration and type, can further improve cooling efficiency. In order to determine the viability of

implementing nanofluids, it is vital to conduct a cost and sustainability analysis. Nanomaterial innovations, such as graphene and carbon nanotubes, present opportunities for enhanced heat transfer efficiency. System-level analysis, comparative studies, and application-specific research will yield insightful information. Additionally, the development of miniaturized, device-specific cooling systems is essential. These research avenues have the potential to significantly advance cooling technologies and optimize thermal management in electronic devices.

### Nomenclature

Al <sub>2</sub> O <sub>3</sub>	Alumina Nanoparticles	MWCNT	Multi-Walled Carbon Nanotube
CFD	Computational Fluid Dynamics	LPM	Liters Per Minute
SiO <sub>2</sub>	Silicon Dioxide	ZnO	Zinc Oxide
mm	Millimeter	Nm	Nanometer
TiO <sub>2</sub>	Titanium Dioxide	Q	Flow Rate (m <sup>3</sup> /s)
A	Cross-Sectional Area Of Flow (m <sup>2</sup> )	V	Average Velocity (m/s)

### REFERENCES

1. M. D. Guidelines, "Express Chipset," no. October, 2007.
2. M. Rafati, A. A. Hamidi, and M. Shariati Niaser, "Application of nanofluids in computer cooling systems (heat transfer performance of nanofluids)," *Appl. Therm. Eng.*, vol. 45–46, pp. 9–14, 2012, doi: 10.1016/j.applthermaleng.2012.03.028.
3. B. P. McGrail, P. K. Thallapally, J. Blanchard, S. K. Nune, J. J. Jenks, and L. X. Dang, "Enhancing thermal conductivity of fluids with nanoparticles," *Nano Energy*, vol. 2, no. 5, pp. 845–855, Oct. 1995, doi: 10.1016/J.NANOEN.2013.02.007.
4. M. Korpyś, M. Al-Rashed, G. Dzido, and J. Wójcik, "CPU heat sink cooled by nanofluids and water: Experimental and numerical study," *Comput. Aided Chem. Eng.*, vol. 32, pp. 409–414, 2013, doi: 10.1016/B978-0-444-63234-0.50069-5.
5. L. Y. Jeng and T. P. Teng, "Performance evaluation of a hybrid cooling system for electronic chips," *Exp. Therm. Fluid Sci.*, vol. 45, pp. 155–162, 2013, doi: 10.1016/j.expthermflusci.2012.10.020.
6. P. Selvakumar and S. Suresh, "Convective performance of CuO/water nanofluid in an electronic heat sink," *Exp. Therm. Fluid Sci.*, vol. 40, pp. 57–63, 2012, doi: 10.1016/j.expthermflusci.2012.01.033. [1]
7. P. Garg, J. L. Alvarado, C. Marsh, T. A. Carlson, D. A. Kessler, and K. Annamalai, "An experimental study on the effect of ultrasonication on viscosity and heat transfer performance of multi-wall carbon nanotube-based aqueous nanofluids," *Int. J. Heat Mass Transf.*, vol. 52, no. 21–22, pp. 5090–5101, 2009, doi: 10.1016/j.ijheatmasstransfer.2009.04.029.
8. Y. Ding, H. Alias, D. Wen, and R. A. Williams, "Heat transfer of aqueous suspensions of carbon nanotubes (CNT nanofluids)," *Int. J. Heat Mass Transf.*, vol. 49, no. 1–2, pp. 240–250, 2006, doi: 10.1016/j.ijheatmasstransfer.2005.07.009.
9. S. Harmand, R. Sonan, M. Faks, and H. Hassan, "Transient cooling of electronic components by flat heat pipes," *Appl. Therm. Eng.*, vol. 31, no. 11–12, pp. 1877–1885, 2011, doi: 10.1016/j.applthermaleng.2011.02.034.
10. S. S. Hsieh, R. Y. Lee, J. C. Shyu, and S. W. Chen, "Thermal performance of flat vapor chamber heat spreader," *Energy Convers. Manag.*, vol. 49, no. 6, pp. 1774–1784, 2008, doi: 10.1016/j.enconman.2007.10.024.

11. A. Briclot, J. F. Henry, C. Popa, C. T. Nguyen, and S. Fohanno, "Experimental investigation of the heat and fluid flow of an Al<sub>2</sub>O<sub>3</sub>-water nanofluid in the laminar-turbulent transition region," *Int. J. Therm. Sci.*, vol. 158, no. September 2019, p. 106546, 2020, doi: 10.1016/j.ijthermalsci.2020.106546.
12. X. Ji, J. Xu, and A. M. Abanda, "Copper foam based vapor chamber for high heat flux dissipation," *Exp. Therm. Fluid Sci.*, vol. 40, pp. 93–102, 2012, doi: 10.1016/j.expthermflusci.2012.02.004.
13. T. E. Tsai, H. H. Wu, C. C. Chang, and S. L. Chen, "Two-phase closed thermosyphon vapor-chamber system for electronic cooling," *Int. Commun. Heat Mass Transf.*, vol. 37, no. 5, pp. 484–489, May 2010, doi: 10.1016/J.ICHEATMASSTRANSFER.2010.01.010.
14. Y. T. Chen, S. W. Kang, Y. H. Hung, C. H. Huang, and K. C. Chien, "Feasibility study of an aluminum vapor chamber with radial grooved and sintered powders wick structures," *Appl. Therm. Eng.*, vol. 51, no. 1–2, pp. 864–870, 2013, doi: 10.1016/j.applthermaleng.2012.10.035
15. H. Hassan and S. Harmand, "3D transient model of vapour chamber: Effect of nanofluids on its performance," *Appl. Therm. Eng.*, vol. 51, no. 1–2, pp. 1191–1201, 2013, doi: 10.1016/J.APPLTHERMALENG.2012.10.047.
16. E. Egan and C. H. Amon, "Thermal Management Strategies for Embedded Electronic Components of Wearable Computers," *J. Electron. Packag.*, vol. 122, no. 2, pp. 98–106, Jun. 2000, doi: 10.1115/1.483140.
17. P. Gauché and W. Xu, "Modeling Phase Change Material in Electronics using CFD - A Case Study," 2000.
18. Y. Kitamura and M. Ishizuka, "Study on chimney effect on natural air cooling of electronic equipment under inclination," *Thermomechanical Phenom. Electron. Syst. -Proceedings Intersoc. Conf.*, vol. 1, pp. 121–127, 2004, doi: 10.1109/ITHERM.2004.1319163.
19. A. N. E. W. Role et al., "A NEW ROLE OF CFD SIMULATION IN THERMAL DESIGN OF COMPACT ELECTRONIC EQUIPMENT ;," 2017.
20. O. Leon, G. De Mey, E. Dick, and J. Vierendeels, "Comparison between the standard and staggered layout for cooling fins in forced convection cooling," *J. Electron. Packag. Trans. ASME*, vol. 125, no. 3, pp. 442–446, 2003, doi: 10.1115/1.1602709.
21. H. Alipour, A. Karimipour, M. R. Safaei, D. T. Semiromi, and O. A. Akbari, "Influence of T-semi attached rib on turbulent flow and heat transfer parameters of a silver-water nanofluid with different volume fractions in a three-dimensional trapezoidal microchannel," *Phys. E Low-Dimensional Syst. Nanostructures*, vol. 88, no. September 2016, pp. 60–76, 2017, doi: 10.1016/j.physe.2016.11.021.
22. A. A. A. Arani et al., "Heat transfer improvement of water/single-wall carbon nanotubes (SWCNT) nanofluid in a novel design of a truncated double-layered microchannel heat sink," *Int. J. Heat Mass Transf.*, vol. 113, pp. 780–795, 2017, Accessed: Jun. 22, 2023. [Online]. Available: [https://www.academia.edu/34584632/Heat\\_transfer\\_improvement\\_of\\_water\\_single\\_wall\\_carbon\\_nanotubes\\_SWCNT\\_nanofluid\\_in\\_a\\_novel\\_design\\_of\\_a\\_truncated\\_double\\_layered\\_microchannel\\_heat\\_sink](https://www.academia.edu/34584632/Heat_transfer_improvement_of_water_single_wall_carbon_nanotubes_SWCNT_nanofluid_in_a_novel_design_of_a_truncated_double_layered_microchannel_heat_sink)
23. J. A. Esfahani et al., "Comparison of experimental data, modelling and non-linear regression on transport properties of mineral oil based nanofluids," *Powder Technol.*, vol. 317, pp. 458–470, 2017, Accessed: Jun. 22, 2023. [Online]. Available: [https://www.academia.edu/33253326/Comparison\\_of\\_experimental\\_data\\_modelling\\_and\\_non\\_linear\\_regression\\_on\\_transport\\_properties\\_of\\_mineral\\_oil\\_based\\_nanofluids](https://www.academia.edu/33253326/Comparison_of_experimental_data_modelling_and_non_linear_regression_on_transport_properties_of_mineral_oil_based_nanofluids)
24. S. M. Hosseini, M. R. Safaei, M. Goodarzi, A. A. A. Alrashed, and T. K. Nguyen, "New temperature, interfacial shell dependent dimensionless model for thermal conductivity of nanofluids," *Int. J. Heat Mass Transf.*, vol. 114, pp. 207–210, 2017, Accessed: Jun. 22, 2023. [Online]. Available:

- [https://www.academia.edu/34584639/New\\_temperature\\_interfacial\\_shell\\_dependent\\_dimensionless\\_model\\_for\\_thermal\\_conductivity\\_of\\_nanofluids](https://www.academia.edu/34584639/New_temperature_interfacial_shell_dependent_dimensionless_model_for_thermal_conductivity_of_nanofluids)
25. M. Afrand et al., "Prediction of dynamic viscosity of a hybrid nano-lubricant by an optimal artificial neural network," *Int. Commun. Heat Mass Transf.*, vol. 76, pp. 209–214, Aug. 2016, doi: 10.1016/J.ICHEATMASSTRANSFER.2016.05.023.
  26. M. Hemmat Esfe, M. Afrand, W. M. Yan, H. Yarmand, D. Toghraie, and M. Dahari, "Effects of temperature and concentration on rheological behavior of MWCNTs/SiO<sub>2</sub> (20-80)-SAE40 hybrid nano-lubricant," *ScienceDirect*, vol. 76, pp. 133–138, Jan. 2016, doi: 10.1016/J.ICHEATMASSTRANSFER.2016.05.015.
  27. M. Asadi and A. Asadi, "Dynamic viscosity of MWCNT/ZnO-engine oil hybrid nanofluid: An experimental investigation and new correlation in different temperatures and solid concentrations," *Int. Commun. Heat Mass Transf.*, vol. 76, pp. 41–45, Aug. 2016, doi: 10.1016/J.ICHEATMASSTRANSFER.2016.05.019.
  28. M. Hemmat Esfe, M. Afrand, S. Gharehkhani, H. Rostamian, D. Toghraie, and M. Dahari, "An experimental study on viscosity of alumina-engine oil: Effects of temperature and nanoparticles concentration," *Int. Commun. Heat Mass Transf.*, vol. 76, pp. 202–208, Aug. 2016, doi: 10.1016/J.ICHEATMASSTRANSFER.2016.05.013.
  29. M. Hemmat Esfe and H. Rostamian, "Non-Newtonian power-law behavior of TiO<sub>2</sub>/SAE 50 nano-lubricant: An experimental report and new correlation," *J. Mol. Liq.*, vol. 232, pp. 219–225, Apr. 2017, doi: 10.1016/J.MOLLIQ.2017.02.014.
  30. A. Asadi, M. Asadi, M. Rezaei, M. Siahmargoi, and F. Asadi, "The effect of temperature and solid concentration on dynamic viscosity of MWCNT/MgO (20–80)–SAE50 hybrid nano-lubricant and proposing a new correlation: An experimental study," *Int. Commun. Heat Mass Transf.*, vol. 78, pp. 48–53, 2016, Accessed: Jun. 22, 2023. [Online]. Available: [https://www.academia.edu/28620012/The\\_effect\\_of\\_temperature\\_and\\_solid\\_concentration\\_on\\_dynamic\\_viscosity\\_of\\_MWCNT\\_MgO\\_20\\_80\\_SAE50\\_hybrid\\_nano\\_lubricant\\_and\\_proposing\\_a\\_new\\_correlation\\_An\\_experimental\\_study](https://www.academia.edu/28620012/The_effect_of_temperature_and_solid_concentration_on_dynamic_viscosity_of_MWCNT_MgO_20_80_SAE50_hybrid_nano_lubricant_and_proposing_a_new_correlation_An_experimental_study)
  31. M. Vafaei, M. Afrand, N. Sina, R. Kalbasi, F. Sourani, and H. Teimouri, "Evaluation of thermal conductivity of MgO-MWCNTs/EG hybrid nanofluids based on experimental data by selecting optimal artificial neural networks," *Phys. E Low-dimensional Syst. Nanostructures*, vol. 85, pp. 90–96, Jan. 2017, doi: 10.1016/J.PHYSE.2016.08.020.
  32. A. Asadi, M. Asadi, M. Siahmargoi, T. Asadi, and M. Gholami Andarati, "The effect of surfactant and sonication time on the stability and thermal conductivity of water-based nanofluid containing Mg(OH)<sub>2</sub> nanoparticles: An experimental investigation," *Int. J. Heat Mass Transf.*, vol. 108, pp. 191–198, May 2017, doi: 10.1016/J.IJHEATMASSTRANSFER.2016.12.022.
  33. S. Sarbolookzadeh Harandi, A. Karimipour, M. Afrand, M. Akbari, and A. D'Orazio, "An experimental study on thermal conductivity of F-MWCNTs-Fe<sub>3</sub>O<sub>4</sub>/EG hybrid nanofluid: Effects of temperature and concentration," *Int. Commun. Heat Mass Transf.*, vol. 76, pp. 171–177, Aug. 2016, doi: 10.1016/J.ICHEATMASSTRANSFER.2016.05.029.
  34. B. Wei, C. Zou, and X. Li, "Experimental investigation on stability and thermal conductivity of diathermic oil based TiO<sub>2</sub> nanofluids," *Int. J. Heat Mass Transf.*, vol. 104, pp. 537–543, Jan. 2017, doi: 10.1016/J.IJHEATMASSTRANSFER.2016.08.078.
  35. R. Agarwal, K. Verma, N. K. Agrawal, R. K. Duchaniya, and R. Singh, "Synthesis, characterization, thermal conductivity and sensitivity of CuO nanofluids," *Appl. Therm. Eng.*, vol. 102, pp. 1024–1036, Jun. 2016, doi: 10.1016/J.APPLTHERMALENG.2016.04.051.

36. E. o. Ila. Etefaghi, H. Ahmadi, A. Rashidi, A. Nouralishahi, and S. S. Mohtasebi, "Preparation and thermal properties of oil-based nanofluid from multi-walled carbon nanotubes and engine oil as nano-lubricant," *Int. Commun. Heat Mass Transf.*, vol. 46, pp. 142–147, Aug. 2013, doi: 10.1016/J.ICHEATMASSTRANSFER.2013.05.003.
37. S. Aberoumand and A. Jafarimoghaddam, "Experimental study on synthesis, stability, thermal conductivity and viscosity of Cu–engine oil nanofluid," *J. Taiwan Inst. Chem. Eng.*, vol. 71, pp. 315–322, 2017, Accessed: Jun. 22, 2023. [Online]. Available: [https://www.academia.edu/34555231/Experimental\\_study\\_on\\_synthesis\\_stability\\_thermal\\_conductivity\\_and\\_viscosity\\_of\\_Cu\\_engine\\_oil\\_nanofluid](https://www.academia.edu/34555231/Experimental_study_on_synthesis_stability_thermal_conductivity_and_viscosity_of_Cu_engine_oil_nanofluid)
38. S. Aberoumand and M. Moravej, "Experimental study on the rheological behavior of silver-heat transfer oil nanofluid and suggesting two empirical based correlations for thermal conductivity and viscosity of oil based nanofluids." Accessed: Jun. 22, 2023. [Online]. Available: [https://www.academia.edu/26335579/Experimental\\_study\\_on\\_the\\_rheological\\_behavior\\_of\\_silver\\_heat\\_transfer\\_oil\\_nanofluid\\_and\\_suggesting\\_two\\_empirical\\_based\\_correlations\\_for\\_thermal\\_conductivity\\_and\\_viscosity\\_of\\_oil\\_based\\_nanofluids](https://www.academia.edu/26335579/Experimental_study_on_the_rheological_behavior_of_silver_heat_transfer_oil_nanofluid_and_suggesting_two_empirical_based_correlations_for_thermal_conductivity_and_viscosity_of_oil_based_nanofluids)